

Reverse Engineering Nature:
Design Principles for Flexible Protection
Inspired by Ancient Fish Armor of *Polypteridae*

by

Steffen H. Reichert

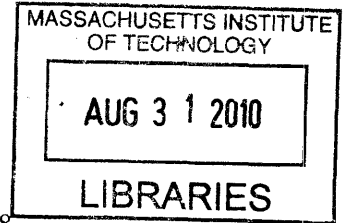
Diplom der Produktgestaltung
Hochschule für Gestaltung Offenbach, Germany, October 2008

submitted to the Department of Architecture
in Partial Fulfillment of the Requirements for the Degree of
Master of Science in Architecture Studies

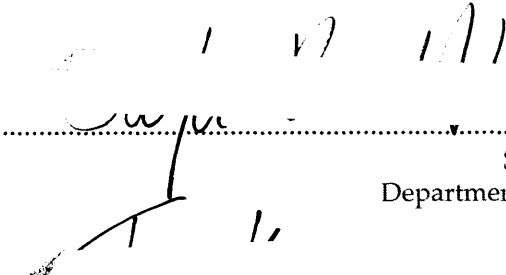
at the

MASSACHUSETTS INSTITUTE OF TECHNOLOGY
June 2010

© Massachusetts Institute of Technology 2010. All rights reserved.



ARCHIVES

Signature of Author 


Steffen Reichert
Department of Architecture
May 19, 2010

Certified by 

Terry Knight
Professor of Design and Computation
Thesis Supervisor

Certified by 

Christine Ortiz
Associate Professor of Materials Science and Engineering
Thesis Supervisor

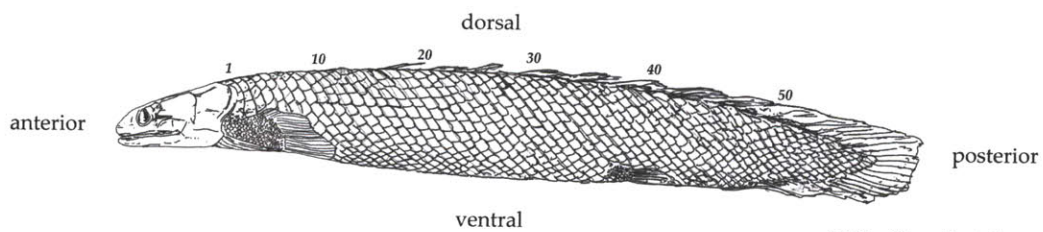
Accepted by 

Julian Beinart
Professor of Architecture
Chair of the Department Committee on Graduate Students

Reverse Engineering Nature:
Design Principles for Flexible Protection
Inspired by Ancient Fish Armor of *Polypteridae*

by

Steffen H. Reichert



© Steffen Reichert

Terry Knight

Professor of Design and Computation
Thesis Supervisor

Christine Ortiz

Associate Professor of Materials Science and Engineering
Thesis Supervisor

J. Meejin Yoon

Associate Professor of Architecture
Thesis Reader

Reverse Engineering Nature: Design Principles for Flexible Protection Inspired by Ancient Fish Armor of *Polypteridae*

by

Steffen H. Reichert

submitted to the Department of Architecture on May 20, 2010
in Partial Fulfillment of the Requirements for the Degree of
Master of Science in Architecture Studies

Abstract

This thesis is about designing structures that combine the dual functions of mechanical protection and flexibility of motion. The structures are inspired by principles observed in the ganoid squamation (scale assembly) of an ancient fish species called *Polypteridae*, which first appeared 96 million years ago. Prior work on *Polypteridae* has focused on understanding the role of the inherent material properties (e.g., stiffness, strength, etc.) of the individual bony scales to provide penetration resistance. Here, geometric design is explored at increasingly larger length scales including 1) morphometric features within individual scales, 2) morphometry of the individual scales as a whole, 3) scale-to-scale interconnections and anisotropic ranges of motion, and, lastly, 4) the entire assembled scale squamation and anisotropic ranges of motion of the entire fish body. Experimental, computational, and mathematical methods employed were micro-computed tomography, microscopy, morphometric analysis, and three-dimensional printing of prototypes. The geometrical design principles discovered were related to biomechanical mobility and protection and then implemented into a generalized, functional design system which possesses similar anisotropic distinctive degrees of freedom and ranges of motion as *Polypteridae*. The design system offers potential for applications in fields of transportation, military, and architecture.

Thesis Supervisor: **Terry Knight**
Professor of Design and Computation

Thesis Supervisor: **Christine Ortiz**
Associate Professor of Materials Science and Engineering

Acknowledgments

First and foremost, I would like to thank my thesis supervisors Professor Terry Knight and Professor Christine Ortiz. Their exceptional support, tremendous guidance, and great encouragement have been invaluable and highly inspiring for me to achieve my goals during my thesis, but also generally during my time at MIT.

Additionally, I would like to express my highest gratitude to Professor Mary Boyce, who has contributed, supported and guided me during my thesis work.

I would like to thank my thesis reader Professor J. Meejin Yoon for her kind input.

Special thanks to my great colleague on the project: Juha Song was not only an excellent work partner but also became a very good friend. Without her collaboration, this thesis would have not been the same.

I would like to thank Professor L. Mahadevan for his fruitful discussions and contributions.

Special thanks to my office mates and very good friends: Skylar Tibbits and German Aparicio, for their inspiration and support. It has been an honor to work side by side with you both.

Thanks to all members of the Design and Computation Group and the Ortiz Group and all my friends who have supported me. Thank you for providing an atmosphere close to that of a family. Forgive me if I do not mention all your names here.

I gratefully acknowledge Prof. Achim Menges, Alex Slocum Jr., Andreas Geiss, Scott Greenwald, Jennifer Burggraf, Chris B. Dewart, Jennifer O'Brian, Kurt Keville, Dr. Bernd Herkner, Simon Schleicher, Objet Geometries Ltd., Materialise Group, for their kind support.

I am thanking our *Polypterus senegalus* specimen for letting me explore his bio-mechanical properties. It was very brave and patient during the anesthetized experiment.

I would like to thank the German National Academic Foundation, Dr. Peter Schaefer from the Peter Schaefer Foundation, and the German Academic Exchange Service for providing me the financial support during my Masters program.

Finally, I want to thank my parents, Hannelore and Gerhard, and my sisters, Kathrin and Christina, and my dear Nicola who have supported me with all their love during this journey.

Table of Contents

Abstract	3
Acknowledgments	4
Table of Contents	6
List of Figures	8
List of Tables	13
Introduction	14
Background	19
Source of Inspiration	20
<i>Scientific Classification of <i>Polypterus senegalus</i></i>	21
<i>Protective Scale Materiality</i>	22
<i>Morphological Features of Individual Scales</i>	24
<i>Global Scale Assembly</i>	28
<i>Flexible Behavior of Scale Integument</i>	33
Theory and Methodology of modelling	34
<i>The Artistry of Modelling</i>	34
<i>Morphometric Analysis of Biological Structures</i>	35
<i>Techniques of Shape Analysis</i>	37
Methods	42
Introduction	43
Specimen and Samples	43
<i>Living <i>Polypterus senegalus</i></i>	43
<i>Skeleton of Dead <i>Polypterus senegalus</i></i>	44
<i>Optical Microscope</i>	45
<i>X-ray Microcomputed Tomography (Micro-CT or μCT)</i>	45
<i>Photography and Motion Picture of Anesthetized <i>Polypterus</i></i>	46
Morphometric Analysis	47
<i>Processing 3D Data and Automated Measurement Techniques</i>	48
Parametric Modelling	49
Strategy of Decomposing the Biological System	50
Prototyping and Fabrication	51

Table of Contents

Results and Discussion	53
Introduction	54
Maximum Body Curvatures of <i>P. senegalus</i>	54
<i>Landmark Identification</i>	57
Global Symmetric Helical Rings	61
Unitizing Scanned Scale Geometry	64
<i>Linear Sections</i>	65
<i>Radial Sections</i>	66
Simplified Anisotropic Scale Assembly Design Model	71
<i>Paraserial Peg and Socket Joint</i>	72
<i>Interserial Overlapping Interface</i>	72
Simplified Scale Assembly	75
Multi-Material Prototyping of the Whole Integument	
Including Connective Tissue	79
<i>Multi-Material Prototype Evolution</i>	83
<i>Final Functional Multi-Material Prototype</i>	87
Table of Abstracted Design Principles	91
<i>Additional Abstraction from Biological System</i>	92
Contributions	94
Future Work	96
Bibliography	98

List of Figures

Figure 1: Drawing of *Polypterus senegalus* (Reichert 2010).

Figure 2: *Polypterus senegalus* specimen (Total body length = 219mm).

Figure 3: The scientific classification of *Polypterus senegalus*.

Figure 4: (A) *P. senegalus* scales consists out of four different composite layers (Bruet et al. 2008). (B) This multilayered composite promotes circumferential cracking patterns that avoid the failure of a whole scale element.

Figure 5: *P. senegalus* scales show very prominent geometric features which have distinctive, performative functions within the scale integument. Peg (P) and Socket (P) joint, axial ridge (AR) area and anterior process (AP). (A) Exterior view and (B) interior view of an individual *P. senegalus* scale (Row 5, 8th scale from dorsal to ventral direction).

Figure 6: (A) In paraserial direction the peg-and-socket joints are supported through (B) collagenous fibers (Sharpey's fibers). (Gemballa and Bartsch 2002) (B-C) Light microscope images from disassembled *P. senegalus* scales, extracted from *P. senegalus* skeleton (Song 2010). (E-F) Two different directions can be described within *P. senegalus* scale armor. Along the paraserial direction scales are connected through a peg-and-socket joint, while along the interserial direction scales simply overlap.

Figure 7: (B-C) Optical microscope images from disassembled *P. senegalus* scales, extracted from *P. senegalus* skeleton (Song 2010). (E-F) Two different directions can be described within *P. senegalus* scale armor. Along the paraserial direction scales are connected through a peg-and-socket joint, while along the interserial direction scales simply overlap.

Figure 8: Underneath the scale integument a fibrous plywood structure (stratum compactum) is connected with every scale of the armor (Gemballa and Bartsch 2002). (is = interserial direction; ps = paraserial direction; asf = interface area between scale and Sharpey's fibers; asc = interface area between scale and stratum compactum; isf = interserial fiber direction; sc = stratum compactum; p = peg; sf = Sharpey's fibers; ap = anterior process).

Figure 9: (A) Helical fiber arrangements around *P. senegalus* bodies (B) Exoskeleton of *P. senegalus*.

Figure 10: (A) Dorsal midline scale shows two socket articulations. (B) Ventral midline scale shows two peg attributes.

Figure 11: (A) *P. senegalus* scales form symmetric mirrored helical rings, which are arranged at an angle between 60° and 45° (Gemballa and Bartsch 2002). (B) A helix can be described as a geodesic line that wanders around a cylinder with a radius (r) and a length (l) and a constant angle (θ). (C) The same cylinder can be represented (unrolled) in two dimensions through an oblong

List of Figures

with the side length (l) and the side length ($2\pi r$). A resulting diagonal (D) results with the angle (θ) represents the helix. (D) The volume (V) reaches its maximum at an angle ($\theta = 55.44^\circ$). (Clark and Cowey 1958)

Figure 12: Skeleton of *Polypterus senegalus*.

Figure 13: (A) Scales rows are directly connected to the fish's spine (Pearson 1981). (B) A ball joint connection between scale armor and ribs allows necessary flexibility (Pearson 1981; Brainerd 1994; Gemballa and Bartsch 2002).

Figure 14: Ball joints between scale armor and dorsal ribs

Figure 15: *P. senegalus* possess a primitive lung. The ventral region allows indentation for breathing.

Figure 16: An anesthetized *P. senegalus* (length = ~219mm), showing very large body curvature

Figure 17: D'Arcy Thompson's theory of transformation.

Figure 18: (A) Exoskeleton of *P. senegalus*. (B) Disassembling and categorization of *P. senegalus* scale integument.

Figure 19: The photographic setup for capturing body curvatures of *P. senegalus* specimen.

Figure 20: Diagram of the followed strategy of decomposing the complex biological design into one main global feature (scale distribution along the body) and two local features (scale-to-scale connections and single scale geometry).

Figure 21: (A) *P. senegalus* in resting position, showing a total length of ~219mm. Excluding the tail fin a body length (L) of ~202mm results. (B-C) Within the XY-plane the *P. senegalus* specimen showed a constant body curvature of ~8%. (D) In the XZ-plane a body curvature of ~29% was measured. (E) Even torsional motion was captured.

Figure 22: 26 Identified Landmarks on an individual scale of *P. senegalus*. Microcomputed tomography was used to measure three dimensional structural data of the scales. This micro-computed tomography was used to generate precise 3D information of the biological forms. (A) Exterior view, (B) interior view.

Figure 23: An automated sectioning script has been developed, exploring the geometry of the interlocking peg-and-socket geometry between two scales of *P. senegalus*.

Figure 24: The resulting geometric outlines of the peg-and-socket geometry. (A) The sectioning in X-direction show the free space between peg and socket. (B) In Y-direction, the scales provide a protective layer with constant thickness including the joint geometry.

List of Figures

Figure 25: The helical, global distribution of scales for *P. senegalus* can be simulated by helix segments. Through mirroring by the XZ-plane, closed symmetrical rings get generated. Last, these rings need to be arrayed along the Y-axis to mimic the helical distribution of the fish armor.

Figure 26: The virtual 3D NURBS model of global, symmetric helical rings in (A) section view and (B) top view.

Figure 27: 3D printed prototype of the monolithic scale row. (A) One single symmetric helical ring. (B) Two true scale rows in assembled configuration. Within the assembly the rings interlock perfectly and constrain all degrees of freedom.

Figure 28: Microcomputed tomography scanning was used to generate 3D mesh information of *P. senegalus* fish scales. The 3D mesh geometry information has been directly used for 3D printed prototypes (1:37.5).

Figure 29: Two neighboring scales have been separated and reassembled into one "unitized" scale geometry that can be assembled to bigger arrangements.

Figure 30: Reverse engineered scales using a linear sectioning technique. Resulting geometry consists out of several NURBS surfaces that have been joined into solid geometry.

Figure 31: Using a radial sectioning technique, it is possible to represent the complex geometry of *P. senegalus* scales through a single lofted NURBS surface.

Figure 32: Detailed images of reversed engineered, 'unitized' *P. senegalus* scales, from (A) exterior and (B) interior perspective. Images (C-F) show 3D printed prototypes using ZCorp 3D printing technology (1: 40).

Figure 33: Virtual 'Unitized' scale assembly from (A) exterior and (B) interior view.

Figure 34: Simplified scale design that can be assembled with rubber bands.

Figure 35: The simplified scale design is designed to allow two rotational degrees of freedom at the (A) paraserial peg-and-socket connection and (B) at the interserial sliding interface. (C) The peg and socket within this design allows two discrete ranges of motion (α , β).

Figure 36: Within the assembly, the scales perform in paraserial direction in two rotational degrees of freedom. Rotational motion around the X-axis is limited by the angled free space between the peg and the bigger socket.

List of Figures

Figure 37: In interserial direction, the overlapping interface allows much more flexibility. Four different degrees of freedom can be explored, two rotational motions (around X- and Z-axis) and two translational motions (along the X- and Y-axis).

Figure 38: Simplified scale assembly in compression state.

Figure 39: Simplified scale assembly in tension state.

Figure 40: Simplified scale assembly in shear state.

Figure 41: Simplified scale assembly in splay state.

Figure 42: Simplified scale assembly in double curvature state.

Figure 43: In the final prototype, morphometric information has served as a basis for the parametric description.

Figure 44: (A) The first step of designing a parametric model of the rhomboidal scales by Polyp-teridae was to define the main geometric features within a two dimensional sketch. The design was highly influenced by the proportions derived from morphometric measurements of the fish scales. (B) In the next step, out of the two dimensional sketch a three dimensional sketch was created. This three-dimensional sketch served as the main geometric framework for the scale design, incorporating many geometric morphological details neglected, e.g. axial ridge, anterior process, and anterior margin, as well as the angled dorsal and ventral surface. (C) In the third step, the three dimensional sketch served as a kind of three dimensional scaffolding to represent the geometry through surfaces. A closed polysurface results and can be converted in solid geometry. (D) Finally, sharp edges have been filleted not only to visually match the biological model, in fact mainly to avoid stress concentrations and cracks at the edges.

Figure 45: The scale geometry was 3D printed using OBJET multi-material printing technology. (A) Two single scales fit perfectly (B) along paraserial axis. (C) A softer material was included in the second prototype which simulated the (D) collagenous fibers (T) between the peg-and-socket joint.

Figure 46: The final virtual assembly incorporating the scale geometry, paraserial collagenous connection, the underlying stratum compactum and the inner soft tissue. (A) Interior view with partially disassembled to show the different layers of the design; (B) from side perspective displaying the overlapping interface with interserial stratum compactum connection; (C) The exterior perspective showing the modular character of the virtual model.

List of Figures

Figure 47: First, a material called TangoBlack was used for the soft tissue layer. This material in combination with a thickness of 17mm, flexibility was very limited. (A) Exterior, (B) interior, and (C) interserial side perspective.

Figure 48: For the second test assembly prototype, the softest material available was used in combination with a material thickness of 3.5mm. Even though the thickness of the printed stratum compactum relates to the actual thickness in the biological model, the system appeared to be to flexible for a large prototype. (A) Exterior, (B) interior, and (C) interserial side perspective.

Figure 49: Last, an additional layer of 3.5mm was added to improve the stiffness of the system. The result was a promising compromise between stiffness and flexibility. (A) Exterior, (B) interior, and (C) interserial side perspective.

Figure 50: The multi-material 2 x 2 test prints show very similar degrees of freedom within the macroscale assemble. (A) Scale assembly in resting position; (B) scale assembly in compression state; (C) scale assembly in tension state. (Compare to Figure 38 and 39)

Figure 51: (A) Scale assembly in shear situation; (B) scale assembly in splay situation; (C) scale assembly performing double curvature. (Compare to Figure 40, 41, and 42)

Figure 52: Final performative, multi-material prototype consisting out of 25 scales (5 x 5 scales assembly). (A) Exterior, (B) interior, (C) and side view.

Figure 53: Final prototype (A) in compression state simulating *P. senegalus* body position with largest body curvature and (B) in tension state simulating the opposite body region while being under large curvature.

Figure 54: (A) Final Prototype performing double curvature. (B) Close-up of exterior scale appearance.

Figure 55: Showing translucency of final prototype from (A) exterior and (B) interior view.

Figure 56: Distorted scale integuments.

List of Tables

Table 1: *Material properties used during multi-material prototyping*

Table 2: *26 Landmarks have been identified, classified and described.*

Table 3: *Table presenting abstracted design principles for application oriented scale assembly designs*

Introduction

Introduction

This thesis focuses on the discovery and understanding of new design principles from the mineralized exoskeleton of the ancient fish *Polypterus senegalus* at multiple size scales. Such design principles may be employed to create a synthetic biologically-inspired mechanically efficient system which can sustain loads while simultaneously retaining flexibility. Flexible and protective structures hold potential for a variety of applications in various fields such as transportation (e.g. ground, air, water, or space), architecture (e.g. building skins or canopies), sports or military (e.g. personal protection), and consumer products (e.g. packaging). (Bruet et al. 2008; Ortiz and Boyce 2008)

Nature offers a nearly unlimited source of inspiration for problems in many fields of research and can lead to unexpected and innovative design solutions. 'Biomimetics' is generally considered as the application of biological methods and systems found in nature to the study and design of engineering systems and modern technology. A thorough understanding of the structure and function of the biological system is first required. Generally, the goal of biomimetics is not to copy the biological system exactly, since such systems function only within a limited range of conditions, but rather, to apply abstracted biological design principles using, for example, different size scales, fabrication techniques and materials. Such abstraction might entail that aspects of a design cannot be captured and must be neglected and, thus, different solutions might occur. (Nachti-gall 2003; Arciszewski and Cornell 2006; Ortiz and Boyce 2008; Krohs and Kroes 2009)

Thorough research and analysis of the biological system should be carried out preceding and in parallel with a biomimetic design process. It is necessary to gain as much knowledge about the inspiring biological system as possible. For designers and engineers, it is especially important so that they can extract the different aspects of the complex design problem, decompose them into sub-components, and reassemble it in a synthetic system (Goodman 1978; Holland 1996). Such studies may include; microstructural and compositional characterization, quantification of material properties (Bruet et al. 2008), morphometric analysis for the assessment of form/shape (Wentworth Thompson 1992; Bookstein 1997; Kendall et al. 1999; Zelditch et al. 2004), and biomechanical analysis of multi-component structures (Gans 1980; Gemballa and Bartsch 2002), all of which are highly connected to function and performance.

Introduction

The design approach in this thesis has focused on creating virtual parametric and physical models of the mineralized exoskeleton of the ancient fish *Polypterus senegalus* (Figure 1). The research and analysis process in understanding the design of this biological system was carried out in parallel with the biomimetic model design. Insight from this analysis influences the direction of the design whereas iterative design, redesign and testing are directed to evolve a system with similar, improved, or tailored behavior relative to the natural model system. During the process of assembling the logical design system, a variety of different aspects need to be balanced at the same time; geometry, material properties and fabrication techniques have to be addressed, sorted, assembled and tested to obtain a desired performance.

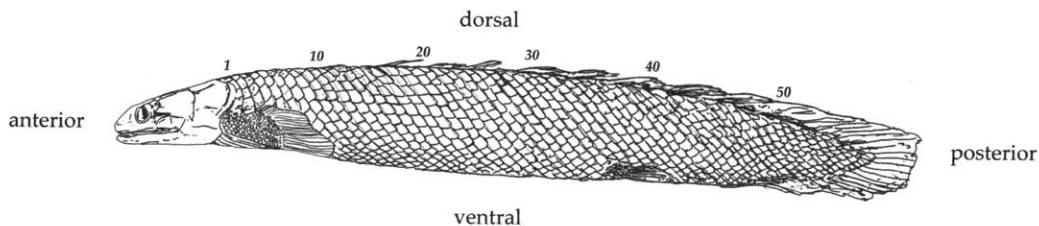


Figure 1: Drawing of *Polypterus senegalus* (Reichert 2010)

The model system chosen for the investigation was the 'living fossil' *Polypterus senegalus*. The *Polypteridae* are a family of ancient fishes that possess a tough, mineralized scale armor (Figure 1). Despite being heavily armored, *Polypteridae* show very agile behavior, and possess the ability to achieve very large body curvatures and high bursts of speed (Gemballa and Bartsch 2002). This dual functionality of protection and flexibility serves as an outstanding source of inspiration. The scales of *Polypteridae* possess an interlocking joint mechanism vertically that limits degrees of freedom and ranges of motion to receive a higher degree of protection. Laterally, scales simply overlap and add more flexibility (Gemballa and Bartsch 2002). This anisotropy in biomechanical behavior was studied and mimicked through synthetic models.

Introduction

In the first chapter, the exoskeleton of *Polypterus senegalus* and its biomechanical features are presented to give the reader a detailed understanding of the complex structure of the model system. Prior work reported in the literature on *Polypteridae* is summarized and includes; material microstructure (Sire 1989) and mechanical functionality (Bruet et al. 2008; Wang et al. 2009) of the individual scales, structural assessment and biomechanical flexibility of the entire scale armor assembly (Pearson 1981; Brainerd 1994; Gemballa 2002). Currently, little is known about the detailed biomechanical mechanisms of the scale armor, in particular how scale-to-scale joint degrees of freedom and ranges of motion, helical scale assembly, and the the interconnecting organic material determine anisotropic macroscopic flexibility. These topics are investigated in the subsequent chapters.

In the second chapter, a description of the methods is provided including; three-dimensional structural quantification via X-ray computed tomography, morphometric analysis, data post-processing (geometry noise reduction, mesh to NURBS conversion), parametric design, monolithic and multi-material three-dimensional printing of synthetic prototypes to produce the complex geometric shapes designed. Furthermore, theoretical and methodological approaches to understand biological design are discussed that serve as a framework for further investigations.

The third chapter includes results and discussion. Morphometric analysis has was to quantify and understand the design of complex biological shapes and their spatial distribution on larger length scales as well as their anisotropic mechanics in an assembled system. The scale-to-scale interconnection geometry was examined to find out how it allows certain degrees of freedom and restricts ranges of motion. Also the arrangement of constituent units into an assembled larger size scale system was explored to interrogate anisotropic flexibility mechanisms, performing differently in specific directions. Extracted morphological information was transferred into a parametric design model. 3D printing proc-

esses including multi-material 3D printing technology were used to fabricate the complex geometric scale parts including their flexible connections. In this way, physical, functional prototypes with anisotropic mechanical behavior were produced. Last, a wide range of design principles is presented in a generalized way to serve as basis for future designs of protective, flexible systems.

Background

Background

Source of Inspiration

Polypterus senegalus belongs to the family of ancient fish *Polypteridae* (bichirs) that are highly predaceous and referred to as “living fossils” with an exoskeletal morphology similar to that found over 96 million years ago (Daget et al. 2001). The genus *Polypterus* lives in various areas in Africa, primarily in flood plains or swampy areas that occasionally dry out. As those areas often have reduced oxygen ratio, *Polypterus* is able to breathe air using a primitive lung, which is another ancestral character of the group. Their prey includes small vertebrates, crustaceans, insects, and fish up to their own size. *Polypterus*' body has a squamation of mineralized ganoid scales.



Figure 2: *P. senegalus* specimens (Total body length = 219mm)

Background

Scientific Classification of Polypterus senegalus

Kingdom	Animalia
Chordata	Phylum
Superclass	Vertebrata
Class	Actinopterygii
Order	Polypteriformes
Family	Polypteridae
Genus	Polypterus
Species	Polypterus Senegalus

Figure 3: The scientific classification of *Polypterus senegalus*

Source: http://www.itis.gov/servlet/SingleRpt/SingleRpt?search_topic=TSN&search_value=161059 (05/05/2010 4:53 PM)

Background

Protective Scale Materiality

The individual scales of *Polypterus* are mineralized and possess a multilayered structure of four different organic-inorganic nanocomposite material layers (Figure 4A) (Sire 1989; Bruet et al. 2008):

Ganoine (1st Outer Layer) is a type of enamel with a highly mineralized non-collagenous structure (Bruet et al. 2008), and an organic content of less than 5% (Ørvig 1967) and a thickness of around 10 μm (Bruet et al. 2008).

Dentine (2nd Layer) possesses less mineral content relative to ganoine and possesses collagenous fibers. Its thickness is measured to be around five times (50 μm) that of the outer ganoine layer (Bruet et al. 2008).

Isopedine (3rd Layer) consists of a 40 μm thick, uniform superimposition of orthogonal collagenous plywood like structure which decreases in mineralization with distance towards the inner surface of the scale (Bruet et al. 2008).

The bone basal plate (4th Inner layer) is the innermost and thickest (300 μm) layer composed of a succession of vascularized bone lamellae. The axis of the collagen fibrils is oriented approximately parallel to the scale surface (Daget et al. 2001).

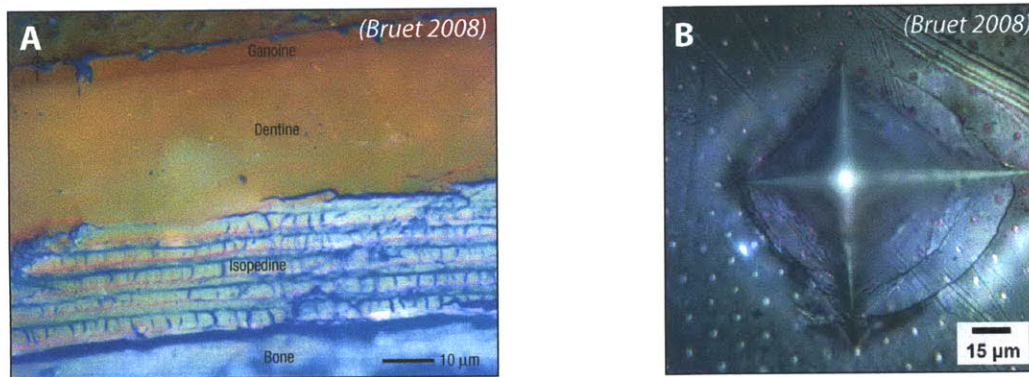


Figure 4: (A) *Polypterus senegalus* scales consists out of four different composite layers. (Bruet et al, 2008) (B) This multilayered composite promotes circumferential cracking patterns that avoid the failure of a whole scale element.

Background

The junctions between layers are functionally graded to promote load transfer and stress redistribution (Bruet et al. 2008). Each material layer has its own deformation and energy dissipation mechanism (Bruet et al. 2008) which leads to the following advantages:

The scales combine the hardness and stiffness of highly mineralized ganoine with the energy dissipation of the underlying dentin layer (Bruet et al. 2008).

Through multilayering it is possible to reduce weight to up to 20% compared to bi-layered composites consisting of ganoine dentine of same thickness while remaining required mechanical properties (Bruet et al. 2008).

Due to the multilayering of materials with different deformation and energy dissipation mechanism, in cases of impact a circumferential cracking mechanism occurs rather than disadvantageous radial cracking (Bruet et al. 2008).

Background

Morphological Features of Individual Scales

Geometry of Individual Scale

Polypteridae possess a squamation, scale armor, integrating rhomboid shaped scales (Figure 5). Within this squamation, most of the body scales show in one direction (X -axis) an interlocking peg-and-socket joint. A pin-like peg (P) articulation fits into a matching socket (S) undercut and constrains the flexibility with this direction. The area between the peg and socket is called the axial ridge (AR) and exhibits the thickest area of each scale. In the direction towards the fish's head, scales have a prominent protruding anterior process (AP). The task of the anterior process may be to direct horizontal locomotion (Gemballa and Bartsch 2002).

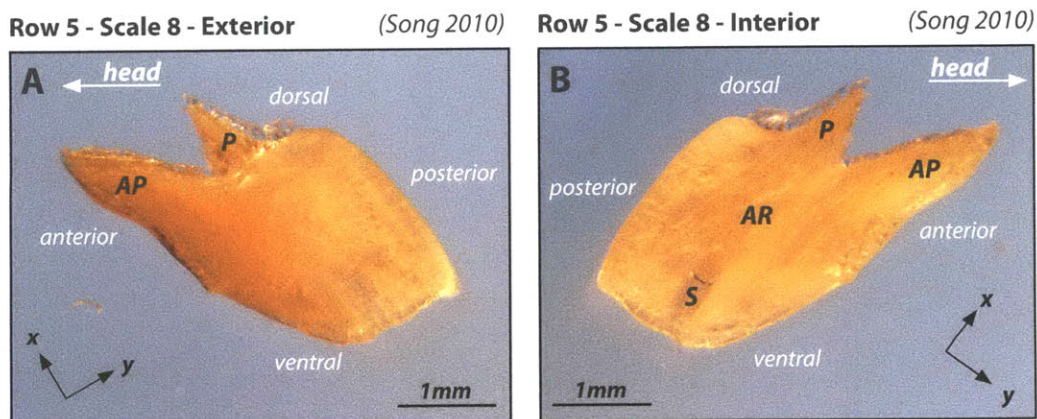


Figure 5: *P. senegalus* scales show very prominent geometric features which have distinctive, performative functions within the scale integument. Peg (P) and Socket (P) joint, axial ridge (AR) area and anterior process (AP). (A) Exterior view and (B) interior view of an individual *P. senegalus* scale (Row 5, 8th scale from dorsal to ventral direction).

Paraserial and Interserial Directions

The scales connect in two very different ways and form therefore two distinguishable directions (Figure 7E-F):

1. *Paraserial interlocking via peg-and-socket joints which form mirrored symmetrical, helical rows*
2. *Interserial (lateral) overlapping interface*

Paraserial

From the dorsal to ventral regions (or vice versa), the scales form helical rows so that each side of the fish shows a symmetric mirrored helix orientation of scales (described in greater detail in following section). The longitudinal or paraserial direction follows parallel to the helical rows (Figure 7A) and shows a very prominent joint, the peg-and-socket joint. The peg, positioned in the dorsal direction fits into the dorsal socket connection and both form a strong and constraining connection in terms of degree of freedom as well as range of motion. In the constrained paraserial connection the peg-and-socket joint is surrounded with an array of connective collagenous fibrils called Sharpey's fibers (Gemballa and Bartsch 2002), presumably for joint reinforcement, support, and alignment purposes. These fibers are intimately connected with the mineral component of the scales.

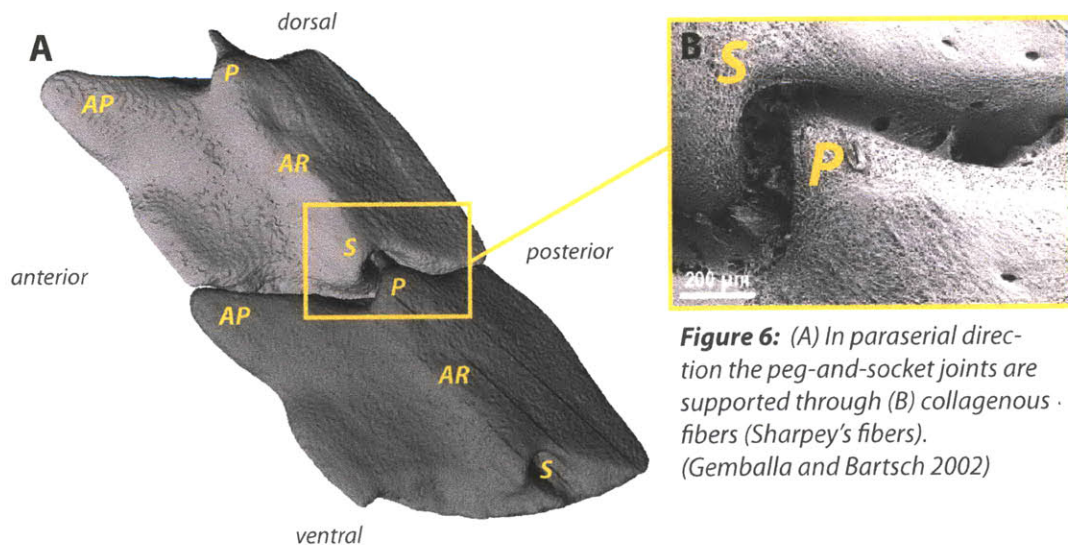


Figure 6: (A) In paraserial direction the peg-and-socket joints are supported through (B) collagenous fibers (Sharpey's fibers). (Gemballa and Bartsch 2002)

Background

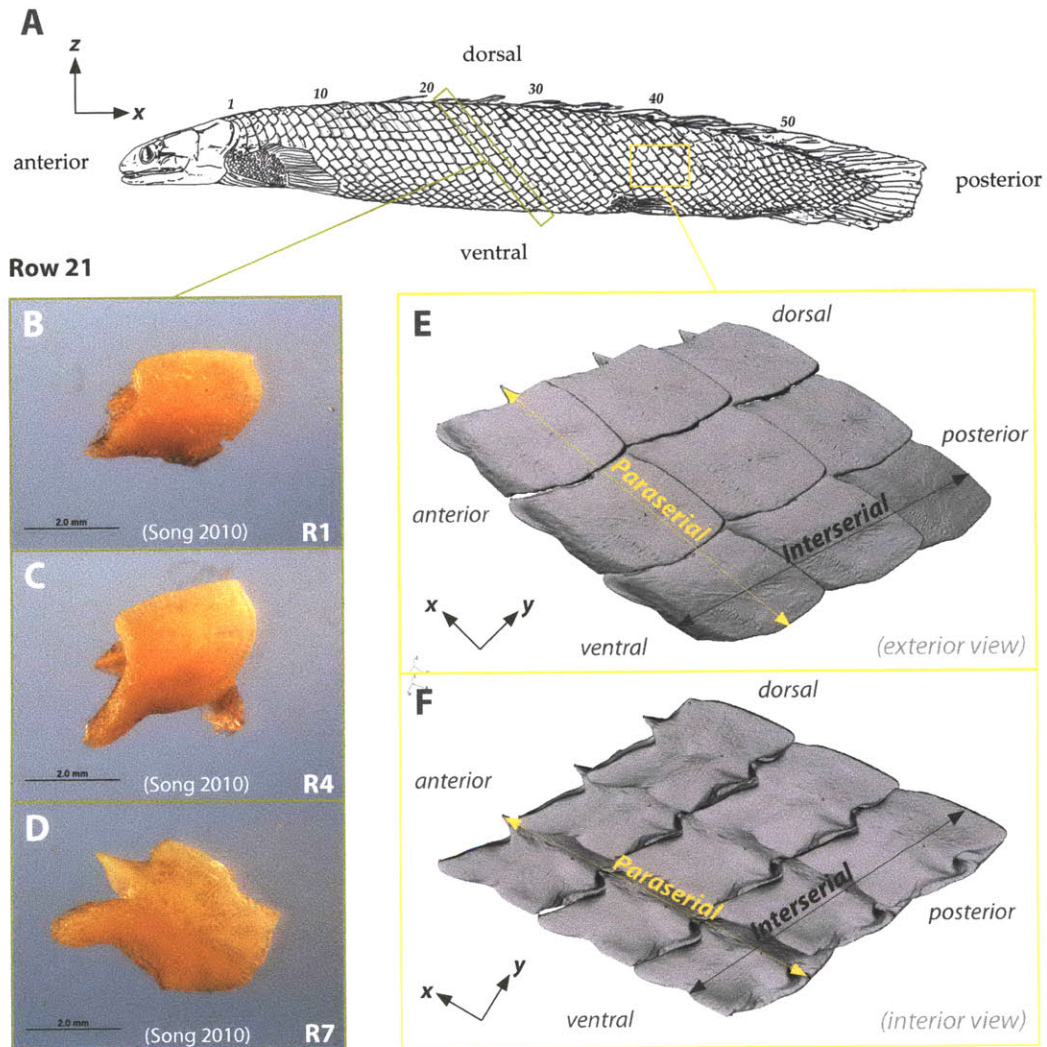


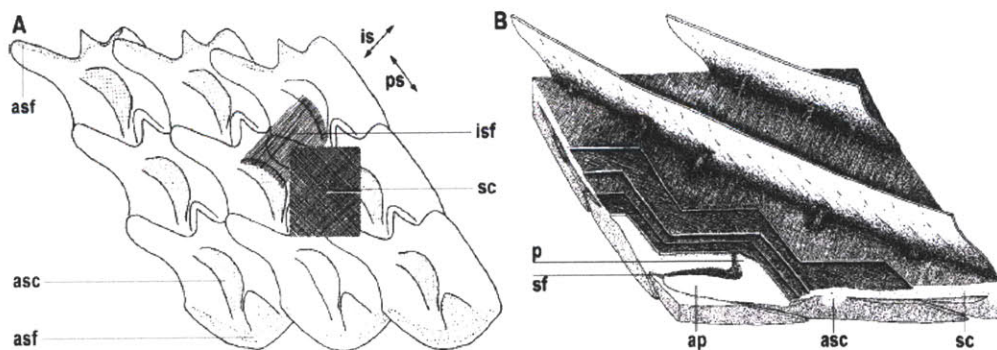
Figure 7:
(B-C) Optical microscope images from disassembled *P. senegalus* scales, extracted from *P. senegalus* skeleton (Song 2010).
(E-F) Two different directions are described within *P. senegalus* scale armor. Along the paraserial direction scales are connected through a peg-and-socket joint, while along the interserial direction scales simply overlap.

Background

Interserial

From the anterior to posterior direction, scales overlap, can slide relative to each other and allow a higher degree of flexibility compared to the paraserial direction (Figure 7E-F). The connection between the scales in this transversal or interserial direction is mainly responsible for the flexibility of the overall scale structure.

Underneath the scales (interior), a plywood-like fibrous layer is wrapped around the fish body (Gemballa and Bartsch 2002). The fibers are arranged paraserially (along helical scale rows) and interserially (lateral between helical rows) (Figure 8A) (Gemballa and Bartsch 2002). This layer supports and interconnects the scale armor as a whole. Each scale is connected to the stratum compactum along their axial ridge (AR) (Figure 6), the thickest cross-section of the scales. The fiber layer spans paraserially but also interserially to the neighboring scales in the squamation. The orientation of fibers changes from anteriorly at an angle of 60° related to the horizontal plane to between 45° - 50° posteriorly (Gemballa and Bartsch 2002). In the literature, it has been postulated that the stratum compactum is the main device in the fish body that provides torsional stiffness (Gemballa and Bartsch 2002).



(Gemballa and Bartsch 2002)

Figure 8: Underneath the scale integument a fibrous plywood structure (stratum compactum) is connected with every scale of the armor (Gemballa and Bartsch 2002). (*is* = interserial direction; *ps* = paraserial direction; *asf* = interface area between scale and Sharpey's fibers; *asc* = interface area between scale and stratum compactum; *isf* = interserial fiber direction; *sc* = stratum compactum; *p* = peg; *sf* = Sharpey's fibers; *ap* = anterior process)

Background

The interesting aspect of the *P. senegalus* scales squamation is that this very protective exoskeleton does not limit its agility. Exploration showed that very small radius body curvatures can be achieved by *P. senegalus*, due to very large body scale overlap during body changes (42-140% in *P. senegalus*) (Gemballa and Bartsch 2002).

Global Scale Assembly

The armor of *Polypteridae* scales rows are arranged in a helical pattern. Starting from the dorsal midline, the scale rows wind geodesically around the body towards the ventral midline (Brainerd 1994; Gemballa and Bartsch 2002). Thus, the squamation can be described as an array of symmetric helical rings (Figure 9A-B), mirrored in *YZ-plane*. Along the dorsal and ventral midline of the fish body, the squamation needs specialized scales that connect the mirrored helical arranged scale rows. Therefore, along the dorsal midline, the connecting scales possess two sockets (Figure 10A) and whereas along the ventral midline, the specialized scales show two peg articulations (Figure 10B).

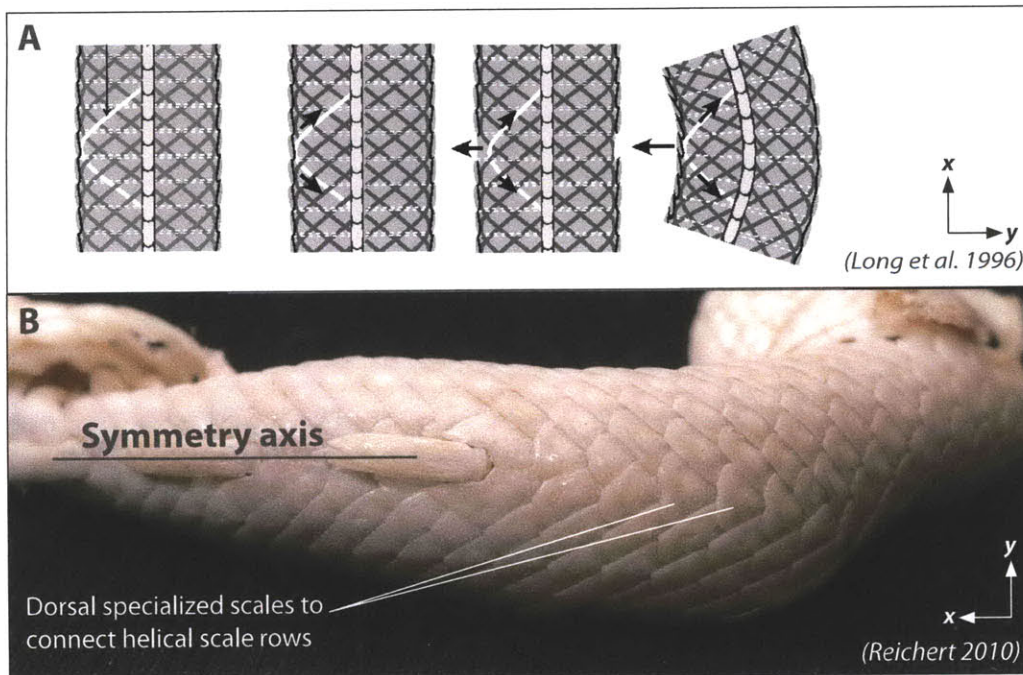


Figure 9: (A) Helical fiber arrangements around *Polypteridae* bodies (B) Exoskeleton of *P. senegalus*.

Background

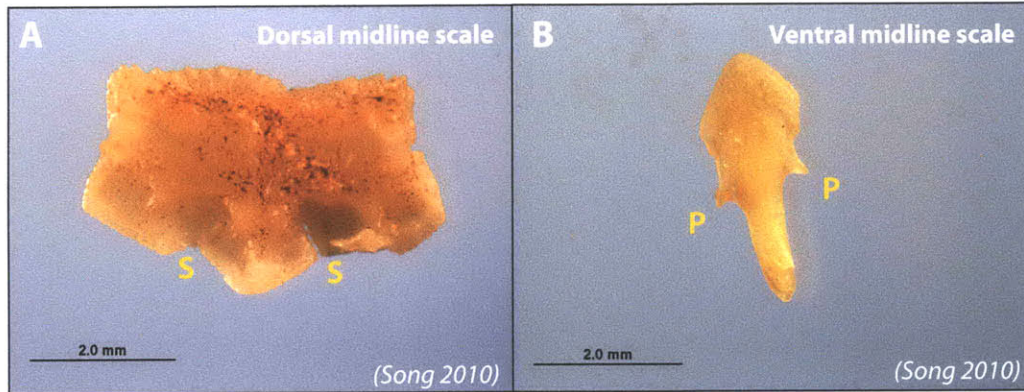


Figure 10: (A) Dorsal midline scale shows two socket articulations. (B) Ventral midline scale shows two peg attributes.

In resting position, the helix-angle (β) (Figure 10A) between the scale rows and the horizontal plane (*XY-plane*) can be measured. The measurements change from anterior region with around 60° to posterior region around 45° (Gemballa and Bartsch 2002). Especially, within the mid region of the body armor an angle of approximately 55° can be measured. During locomotion, the helix-angle (β) changes with increasing body curvature.

The helical systems with an angle of 54.44° perform quite differently compared to helical systems. In literature (Figure 11B), the helical fibrous skin of worms has been examined (Clark and Cowey 1958). A helix with a length D (Figure 11C) achieves the highest volume, if the angle between the helix and the horizontal plane approaches 54.44° (Figure 11D) (Clark and Cowey 1958). In resting position, worms have a circular cross section. The cross section becomes elliptical with the changing the worm's body curvature and at the same time the volume of the body decreases (Clark and Cowey 1958). As a result, a helix with 54.44° allows an optimal resting position with the most volume. With increasing and decreasing angle the volume decreases. A decreasing volume of the fish compresses the internal tissue which produces a counter force against the motion. Therefore, a 54.44° is an ideal angle for tubular structures. Modern hose designs use a 54.44° counter-helical fiber reinforcement to ensure the best water flow within a curved hose.

Background

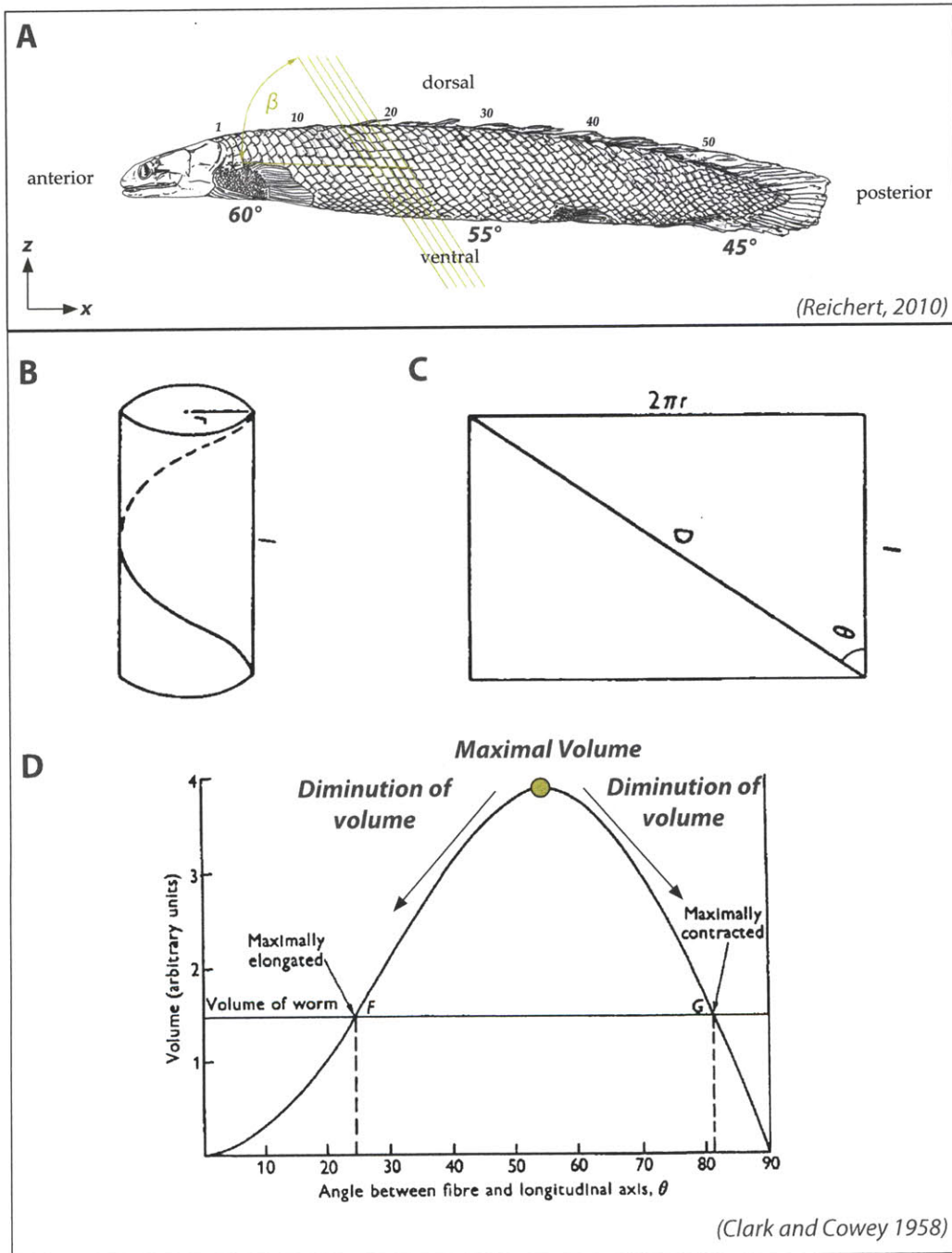


Figure 11: (A) *P. senegalus* scales form symmetric mirrored helical rings, which are arranged at an angle between 60° and 45° (Gemballa and Bartsch 2002). (B) A helix can be described as a geodesic line that wanders around a cylinder with a radius (r), a length (l) and a constant angle (θ). (C) The same cylinder can be represented (unrolled) in two dimensions through an oblong with the side length (l) and the side length ($2\pi r$). A resulting diagonal (D) results with the angle (θ) represents the helix. (D) The volume (V) reaches its maximum at an angle ($\theta = 55.44^\circ$). (Clark and Cowey 1958)

Background

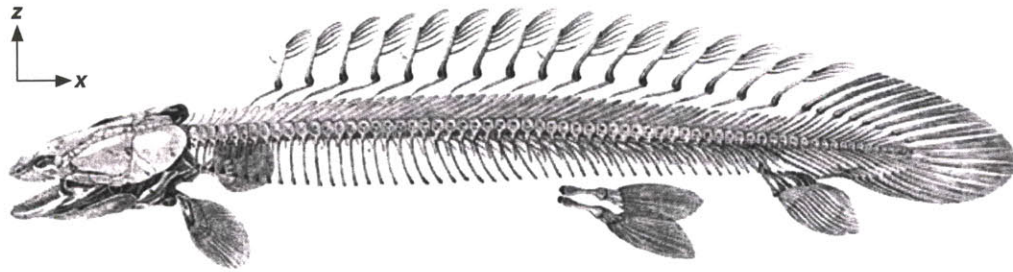


Figure 12: Skeleton of *Polypterus senegalus*

(Filler 2007)

P. senegalus possesses vertebral spine with ventral but also dorsal ribs (Figure 12) (Britz and Bartsch 2003). The dorsal ribs are connected with the scale squamation through ball joints. Additionally, a horizontal septum exists along the whole body of *Polypteridae* (Gemballa and Bartsch 2002) connecting the vertebral spine with the scale armor. A ball joint (BJ) between the rib (R) and the scale allows a flexible connection allowing all three rotational degrees of freedom (Figure 13, 14). It can be assumed that the most important reason for a connection between the ribs and the scale integument is prevention of compression. The ribs will stiffen the helical rings to resist deformation into the fish.

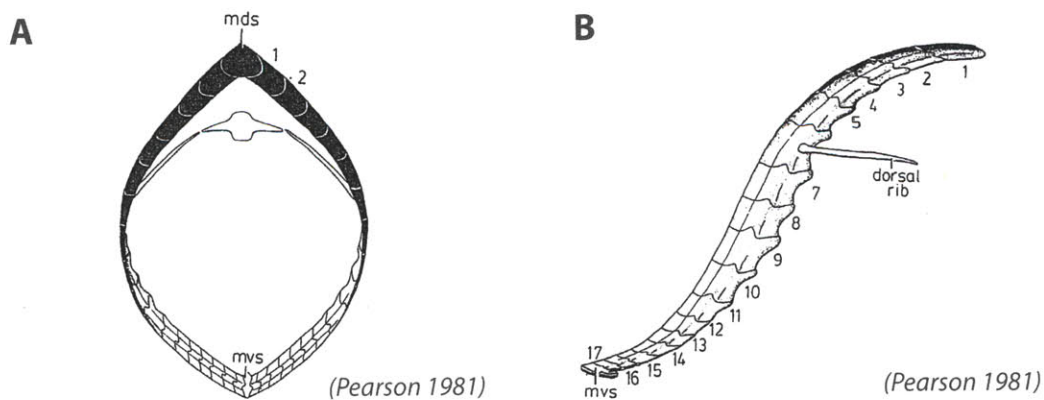


Figure 13: (A) Scales rows are directly connected to the fish's spine (Pearson 1981). (B) A ball joint connection between scale armor and ribs allows necessary flexibility (Pearson 1981; Brainerd 1994; Gemballa and Bartsch 2002).

Background

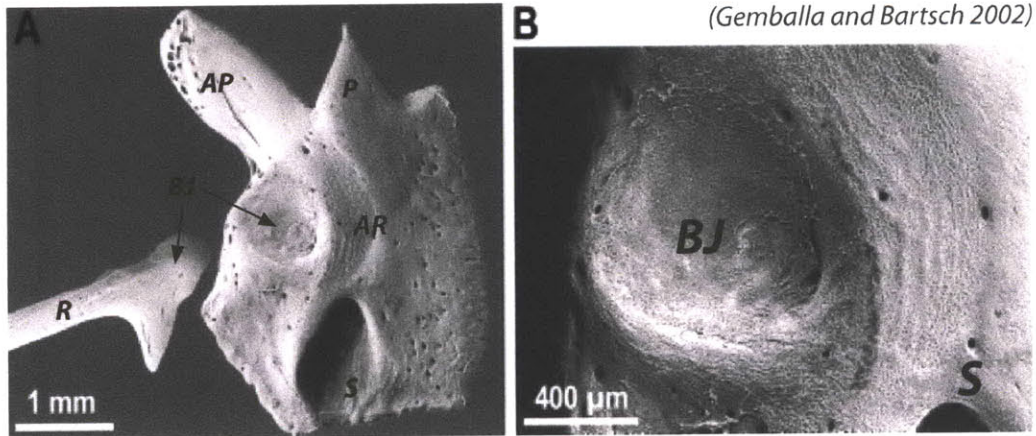
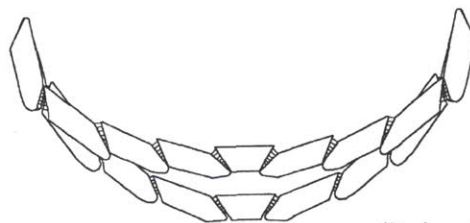


Figure 14: Ball joints between scale armor and dorsal ribs

The *Polypterus*' integument of interlocking rhomboid scales is known to deform during respiration. This shape change results in the ventral integument being deformed in compression (Brainerd 1994). The geometry of scales and collagen fibers within the skin converts compressive strain to tensile strain, thus storing energy in collagen fibers in tension (Brainerd 1994). Active exhalation, caused by contracting muscles in the lung wall (Brainerd 1994), compresses the bony scale jacket (Brainerd 1994) and the body volume of the fish decreases. When *Polypterus* is at rest, its integument is circular in cross-section and the overlapping scale edges are parallel. During exhalation, the hemispherical shape of the ventral integument is deformed, the scales rotate slightly (Brainerd 1994) and the integument flattens on the bottom. The scales act as small levers that stretch the collagen fibers between them as soon as their edges become non-parallel (Brainerd 1994). Inhalation occurs when the scale jacket recoils to its original shape (Brainerd 1994). When the fish opens its mouth to inhale, the stretched fibers return to their original lengths and pull the scale jacket back into a circular shape, thus sucking air into the lungs.



(Brainerd 1994)

Figure 15: *P. senegalus* possesses a primitive lung. The ventral region allows indentation for breathing.

Background

Flexible Behavior of Scale Integument

As with most fishes, *Polypteridae* propel through a series of roughly S-shaped curves that shift tailwards. (Gans 1980) Concavities are produced by a shortening of the muscles (of the concave side); the stimuli pass alternately along the two sides of the spinal cord, producing alternating waves or contractions along the sides of the trunk. In the literature it has been proposed that the ganoid scales of *Polypteridae* do not especially limit body curvature, act as torsion resisting devices, but damp torsion together with the stratum compactum and internal body pressure. (Gemballa and Bartsch 2002)

Experiment: Juha Song
Photography: Steffen Reichert



Figure 16: An anesthetized *P. senegalus* (length = ~219mm), showing very large body curvature.

Theory and Methodology of modelling

The Artistry of Modelling

“Historically and traditionally, it has been the task of the science disciplines to teach about natural things; how they are and how they work. It has been the task of engineering school to teach about artificial things: how to make artifacts that have desired properties and how to design.” (Simon 1996)

Modelling is a very important part of science and engineering as well as of architecture and design, as it describes the world through simplified systems. According to systems theory (Bertalanffy 1976; Holland 1996), a model never captures the source world as a whole, but it can describe certain specific aspects with a degree of repeatability. The relationships within the system help us to understand how things work around us.

In this thesis, I try to bridge the rigorous scientific description with the ability of ‘embedding’ (Stiny 2008) analyzed phenomena into a logical design model, transferring a natural into an artificial system (Simon 1996). The goal lies in understanding the main design principles of a biological system and proving them through a physical functional model. Nelson Goodman (1906-1996), an American philosopher, wrote in his work “Ways of Worldmaking” (Goodman 1978) about the different methods of model making. According to Goodman, five processes are needed to create a model:

1. *Decomposition and Composition*
2. *Weighting*
3. *Ordering*
4. *Deletion and Supplementation*
5. *Deforming*

Background

These main processes during model making formed the methodological basis for the following design investigations as well as the analysis interpretation. During analysis, basic elements and their relationships within a system can be extracted through *decomposition*. Different perspectives on a system allow identifying different elements and different relationships within the same system. All of them can be *composed* into a synthetic system again. The elements and their relationships need to be *weighted* and placed in hierarchical *order*. Through *deletion* and *supplementation* the system can be adjusted. Finally, manipulation of parameters (*deformation*) can be used to utilize the system and transfer it to different contexts.

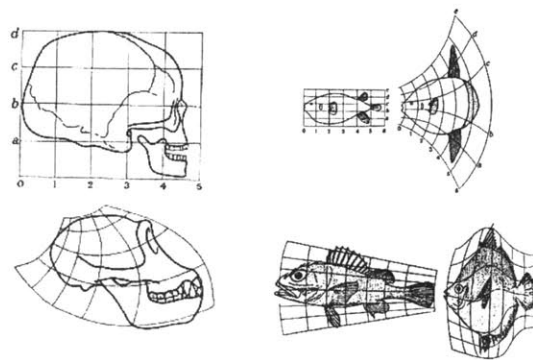
Morphometric Analysis of Biological Structures

In biological organisms, we can usually discover very complex forms, deriving from and changing through complex cause to provide required functionality. Hence, there is a tight relationship between an organism's form and its performance.

D'Arcy Thompson (1860-1948) was one of the few voices in his time who reminded biologists that evolution and developmental biology, the two great processes of creation are deeply intertwined. (Arthur, 2006) The philosophy that pervades "On Growth and Form", and indeed D'Arcy Thompson's publications in general, is the explanation of natural phenomena in terms of physical, and especially mathematical, laws. (Arthur, 2006) His mathematical approach to biological transformation was entirely novel among biologists; and it is still in the present day. No one so far had attempted to show that the differences between the forms of related species can be represented geometrically. Although D'Arcy Thompson did not see biochemical and biomathematical approaches as antagonistic, he encouraged biologists to place less emphasis on matter and more on the forces that shape it. (Arthur, 2006)

"We pass quickly and easily from the mathematical concept of form in its static aspect to form in its dynamic relations. We rise from the conception of form to an understanding of the forces which gave rise to it; and in the representation of form and in the comparison of kindred forms, we see in the one case a diagram of forces in equilibrium, and in the other case we discern the magnitude and the direction of the forces which have sufficed to convert the one form into the other. Here, since a change of material form is only effected by the movement of matter, we have once again support of the schoolman's and the philosopher's axiom: Ignorato motu, ignoratur Natura." (Thompson, 1992)

His theory of transformation makes use of the Cartesian grid (Figure 17), drawn to the background of the outlines of animals or plants, which can be systematically submitted to mathematical transformation (e.g. stretching or distortion). The transformed outline is then compared to the original. By taking two or more related forms, it can thus be determined whether one could be produced from the other by simple transformation.



(Thompson 1992)

Figure 17: D'Arcy Thompson's theory of transformation

Through the superimposition of stretched and distorted Cartesian grids, D'Arcy Thompson was able to describe relationships between similar complex biological shapes. The difference between the grids, he describes as the forces that shaped/changed the object.

Techniques of Shape Analysis

In modern biology, the analysis of shape and shape difference still plays an important role (Zelditch et al. 2004). Analysis of shape or differences between shapes can be explored between individuals or parts of individuals and can provide insight into processes of growth and morphogenesis, functional roles or responses to the selective pressures (Zelditch et al. 2004). But studying biological shape entails many difficulties. Starting with simple measurements, most biological shapes show very curved and rounded, to designer's and engineer's description, 'freeform' geometry. Without a blueprint of their generation, the understanding, description and interpretation of geometric features can be difficult. Additionally, problems with perspective of imaging and phenotypic discrimination between samples handicap extracting exact geometric information, and quantifying biological shapes. But exactly those measurements allow capturing functional, systematically and developmentally important characters of the organism as well as its size and shape (Zelditch et al. 2004).

"In fact, any application where the geometrical comparison objects is required will require the use of shape analysis." (Dryden 1999)

The origin of morphometrics lies in mathematical shape analysis and statistics, all fields that need to compare geometric objects are required for shape analysis. Therefore, geometric morphometrics are already used in very different fields like archeology, biology, chemistry, geography, image analysis, medicine and engineering (Dryden 1999). The most important pioneers of the subject of shape analysis are David G. Kendall and Fred L. Bookstein (Dryden 1999). Kendall proposed in his shape theory that the essence of geometric shape can very precisely defined as *"all the geometric information that remains when location, scale and rotational effects are filtered out from an object"* (Kendall 1977). This decomposition of shape information and registration information is an interesting approach to understand the complex design of biological shape.

Shape information

The complexity of shapes needs to be decomposed into much simpler components. In general, there are several ways to represent shapes in geometric terms:(e.g. solid volumes, mathematical surfaces, polygonal surface meshes, section curves or point clouds). Morphometrics utilizes the simplest geometric objects, landmark points, to capture the complex geometry of biological shape. Landmark points are distinct anatomical loci that can be identified in all specimens (Zelditch et al. 2004). Compared to previous morphometric measurement techniques, landmark data offer much richer information as numerous different analysis techniques can be applied. Since landmark points serve as the basis for morphometric analysis their identification is of high importance for the result of the analysis. To provide an informative representation of a complex biological form, certain consideration for choosing landmarks have been followed (Zelditch et al. 2004):

1. Consistency of relative position:

To compare similar shapes it is important that all specimens share common features which are comparable. Too different shapes will blur the results (Zelditch et al. 2004).

2. Adequate coverage of form:

It is important to place landmarks in a rigorous way so that most geometric features are covered. Placing suitable landmark data that archives a specific biological shape series needs a special type of artistry. Most of the geometric differences have to be already identified to be able to place the right number and the right location. In other words, even before starting the analysis of biological shape using landmark points, a high understanding of the shape is needed and the importance of certain geometric featured must be 'embedded' (Stiny 2008). Additionally, it is advisable to place a slightly higher number of landmark points to open up a space for unexpected results (Zelditch et al. 2004).

Background

3. Repeatability:

All landmarks need to be reliably found in all specimens, otherwise the accuracy of the results decreases dramatically (Zelditch et al. 2004). Depending on the source type of data and the clarity of identification, the size of errors can be big or sometimes surprisingly small and appear in only one or sometimes in multiple dimensions. For that reason it is desirable to identify specific geometric features that can easily and reliably be found on any specimen, like e.g., tips of a shape, geometric inflection points, etc.

Registration information

The registration information of the location, size and orientation of the object may be of changing interest according to the application of the analysis (Dryden 1999). For example, to calculate an average shape or the variability in shape in a population of objects, their location and orientation might be of low interest (Dryden 1999).

Registration information can be removed from two pairing objects by superimposition techniques, e.g. generalized procrustes analysis. Based on landmark data, the generalized procrustes analysis allows extracting location, size and orientation information from an object.

Translation:

To remove location errors between two shapes the centroid point of each shape needs to be calculated. Through summing all X-values, all Y-values and all Z-values of all landmark coordinates of a shape data set and the calculation of the mean value for each dimension, the centroid point for each shape can be determined. If then the centroid gets subtracted from each landmark point, the shape gets centered on the world coordinate origin. The calculated centroid point can be thus also seen as a translation vector.

Background

Scaling:

After being centered, each landmark with a shape data set can also be interpreted as a size vector starting at the new centroid point, which is also the origin of the world coordinate system. By adding up all X-, Y-, Z-values of all landmarks and calculating the mean value of all these dimensional components of all landmarks, the centroid size of an object results. This centroid size contains the generalized size component of an object. Through dividing each dimensional component (X, Y, Z) by the centroid size value, the size component of the shape can be removed, and a unitized, size independent, shape remains.

Orientation:

The last step of aligning a landmark data set with each other, is removing rotational errors. According to the Euler's rotation theorem, three-dimensional rotation can be performed using only three angles (Weisstein 2010). By calculating the mean rotational angle for each of the three angles the rotational error can be removed.

Visualization of shape analysis

The visualization of results should be created with value. A specialized visualization influences the viewer's perspective and the interpretation of information but communicates clearly the intentions of an analysis. On the other hand more open visualization might give more freedom to find unexpected results. In morphometrics, several kinds of data visualization are used. The most common and most visually pleasing is the thin plate spline. A thin plate spline basically represents a distorted coordinate grid, deformed through the differences in shape between two shape data sets. One data set will be defined as a reference and a Cartesian grid is superimposed. Differences in shape between two objects can be emphasized if now the grid of the second shape gets warped according to the

Background

differences in shape. These differences can be calculated as a bending matrix. A bending energy value results as a side product.

Landmark typology (Bookstein, 1991)

Type 1: Landmarks of type 1 are optimal definable landmarks with discrete positions (Zelditch et al. 2004). They can be clearly identified on a shape with only minimal possibilities of error and independently from other landmarks. They indicate most of the time directions of growth and forces within a shape (Zelditch et al. 2004).

Type 2: Landmarks of type 2 are more problematic. They can contain a higher possibility of error and are sometimes related to other landmarks within a shape data set (Zelditch et al. 2004). For example, local minima or maxima or curvature can be described by type 2 landmark points.

Type 3: Landmarks of type 3 are the most unreliable landmarks and should only be considered carefully within a data analysis. They are very difficult to identify on a shape and therefore can contain a high value of deviation. Still they can be important to describe tendencies of shape .

Tools of geometric shape analysis have remarkable advantages over traditional measurement methods, offering precise and accurate description of shape, and comprehensible visualization methods for interpretation and communication of results (Zelditch et al. 2004).

Methods

Introduction

In this chapter, all used methods and techniques are presented in detail. First, measurement and imaging techniques to understand and quantify the complex biological shapes and their behavior are addressed. The analysis starts with traditional measurement techniques and continues with X-ray computed tomography imaging to capture three-dimensional information in combination with advanced morphometric analysis procedures. To convert, manipulate, and quantify the derived three-dimensional geometric data custom scripts were developed that automate specific processes. For the process of design, a parametric modelling environment has been chosen to generate a logical associative geometric model. Monolithic and multi-material three-dimensional printing technologies were used to fabricate the complex geometric of the design models.

Specimen and Samples

Living Polypterus senegalus

A living *Polypterus senegalus* (total length including tail fin ~219 mm, body length ~202 mm) was employed for body curvature measurements. The *P. senegalus* is maintained in a freshwater aquarium with water kept at ~26°C and a pH of ~7. The *P. senegalus* is fed regularly with dry fish food. The fish was purchased at Tropic Isle Aquarium Store (4 Pierce Street, Framingham, MA). All experiments were performed in accordance with federal guidelines and regulations and approved by the MIT Committee on Animal Care (Protocol 0707-056-10) and the fish recovered well from the anesthesia. MIT has an Animal Welfare Assurance on file with the Office for Laboratory Animal Welfare (Assurance number A-3125-01). For the body curvature measurements and scale removal surgery, the living *P. senegalus* was anesthetized and a row of four scales surgically dissected off from the 49th row on the left flank (posterior region). Tri-

Methods

canemethanesulfonate (MS-222, Sigma-Aldrich) was used for general anesthesia, prepared at a concentration of 1.6 g/500 mL H₂O with 3 pellets of KOH for neutralization. The fish was subsequently removed and immersed in a mixture of 50 / 50 MS-222 and water from the tank to maintain anesthetization. (Bruet, 2009) Experiments were performed in collaboration with Juha Song (PhD candidate, DMSE, MIT).

Skeleton of Dead Polypterus senegalus

Optical microscopy was employed to image the scales extracted from the skeleton of a dead *P. senegalus* (total body length of ~150 mm) (Figure 18A-B). The skeleton was stored under ambient conditions. Experiments were performed in collaboration with Juha Song (PhD candidate, DMSE, MIT).

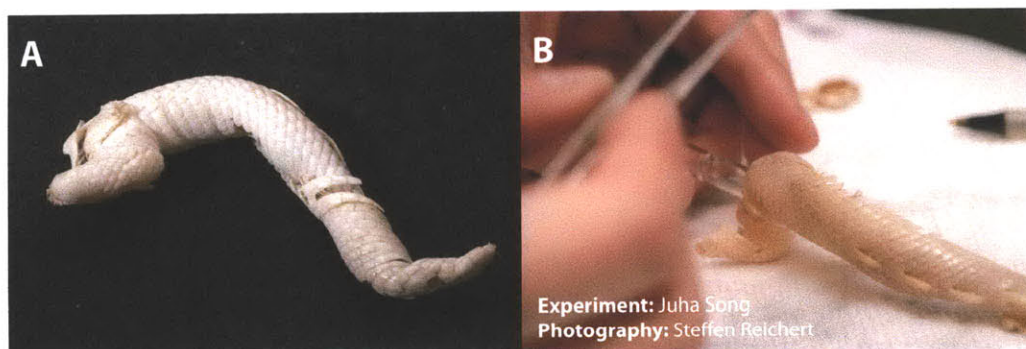


Figure 18: (A) Exoskeleton of *P. senegalus*. (B) Disassembling and categorization of *P. senegalus* scale integument.

Imaging

Optical Microscope

A stereo microscope (Olympus SZX2, Tokyo, Japan) was used to image the *Polypterus senegalus* scales from the different positions of the body. Experiments were performed in collaboration with Juha Song (PhD candidate, DMSE, MIT).

X-ray Microcomputed Tomography (Micro-CT or μ CT)

The *Polypterus senegalus* scales were scanned using Micro-CT (μ CT) system (Viva CT40, Scanco Medical AG, Switzerland) operated at 45 kV and 177 μ A. Microtomographic slices were recorded every 12 μ m and were reconstructed with $12 \times 12 \mu$ m voxels (volume elements) in plane. A constrained three-dimensional (3D) Gaussian filter ($\sigma = 0.8$ and support = 1) was used to partially suppress noise in the volumes. Moreover, the three-dimensional geometric information of the scanned samples was converted into three-dimensional polygonal meshes (stereo-lithography - STL, bilinear and interplane interpolation algorithm) using an interactive medical image control system (MIMICS 9.0, Materialise, Belgium). The converted STL file was imported into a CAD (Computer-aided design) software (RHINOCEROS®, Robert McNeel and Associates, USA). Experiments were performed in collaboration with Juha Song (PhD candidate, DMSE, MIT).

Methods

Photography and Motion Picture of Anesthetized Polypterus

For photographic imaging of the anesthetized fish curvature measurements, a Nikon D90 D-SLR camera with HD video capabilities was used in combination with a Nikon AF-D 60mm f2.8 Makro lens. All images were captured in NEF (RAW) format and converted using Adobe Photoshop Camera RAW software. For constant light conditions a LOWEL TOTA camera light set was used. Experiments were performed in collaboration with Juha Song (PhD candidate, DMSE, MIT).

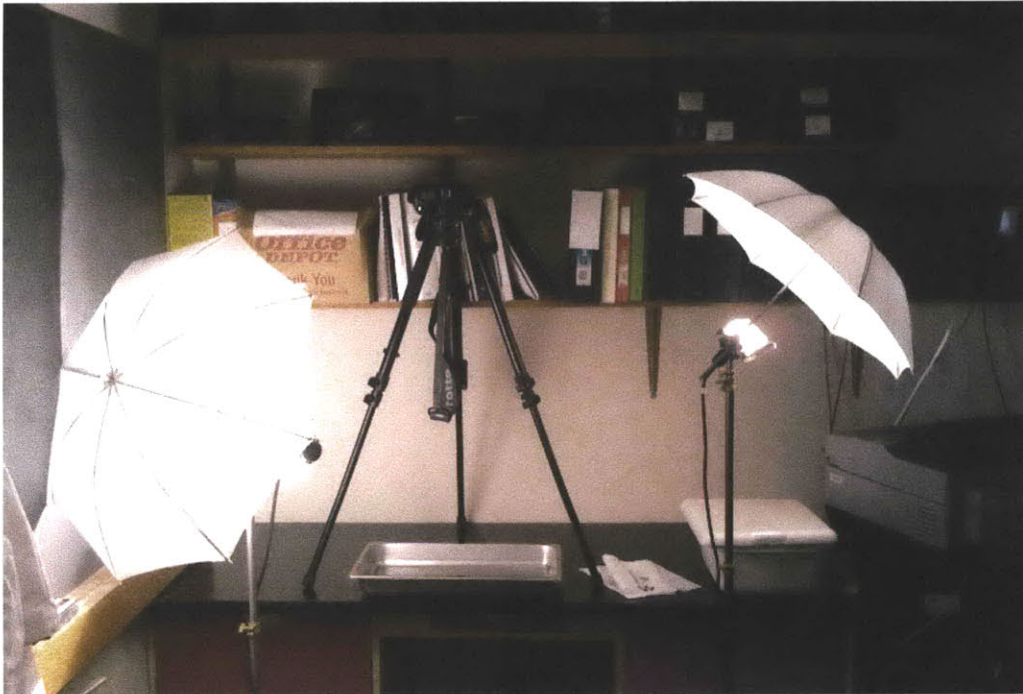


Figure 19: The photographic setup for capturing body curvatures of *P. senegalus* specimens.

Morphometric Analysis

Microcomputed tomography data (DICOM file format) was converted into 3D mesh geometry and served as basis material for the morphometric analysis. In this thesis, the emphasis was focused on the outer surface of the object, but microcomputed tomography is also able to capture detailed internal information which can be useful for further analysis. In this study, analysis scripts have been developed with a standardized CAD software (RHINOCEROS®, Robert McNeel and Associates, USA) that allows the use of 3D manipulation methods for noise removal and post-processing 3D mesh data.

Morphometric quantification of shape has been explored in this thesis to understand the geometry of *P. senegalus* scales. By placing landmarks, registration points, on prominent geometric locations attempt to capture the special geometric features, a detailed understanding of the geometry emerges. Variations in shape allow interpretation of form in relation to function. The scales of *P. senegalus* show variations in shape along the whole body (Gemballa et al, 2002). Morphometric analysis allows quantifying the differences, visualizing the differences and informing mechanical design. Geometric morphometrics has directly informed the design in this thesis in two ways - unitized scale deformation or parametric variation. The first strategy is based on a unitized scale design. One scale can be selected as reference geometry. Through 3D deformation techniques these scales can be deformed into basically any shape. With the help of landmark data, these deformations can be controlled so that variation in shape can be interpolated.

The second way to inform design by morphometric information is to utilize landmark points to extract information about proportion for parametric models. With a hierarchical constructed parametric model that incorporates landmark locations the information of differentiation can be included by calculating proportions.

Methods

Both strategies allow the production of prototypes which closely represent the fish squamation due to the integration of differentiation derived from geometric morphometrics. The prototype can then be fabricated and its mechanical behavior tested. The resulting performance can be mapped back to the differentiated geometry to give a better understanding about the relationship between form and function.

Processing 3D Data and Automated Measurement Techniques

For post-processing and manipulation of 3D data derived from microcomputed tomography scans, a standard computer-aided-design (CAD) software (RHINOCEROS®, Robert McNeel and Associates, USA) package was used. This type of CAD software package offers a wide range of import and export functionality including STL (stereo-lithography - STL, bilinear and interplane interpolation algorithm) file support to transfer 3D information between several software packages. Finally, RHINOCEROS 3D® has been used to prepare the scanned 3D mesh geometry for 3Dprinting fabrication machines. With this process of preparation, the geometry was scaled, oriented and analyzed for closeness to avoid failure during the rapid prototyping process. Certain measurements techniques have been automated using the RHINOCEROS 3D® scripting interface (Rhino-script based on VBScript programming environment).

Parametric Modelling

During the design process geometric features were defined in a parametric model. A parametric computer-aided-design (CAD) software (SOLIDWORKS®, Dassault Systèmes SolidWorks Corp., France) was used. Parametric modeling enables the construction of hierarchically associated, variable design models. Each geometric element contains defined relationships to other geometric elements. Due to these relationships, it is possible to change the proportions of the design model easily. This allows the generation of a wide range variations. The 3D geometry can be exported in various files formats including STL format for 3D prototyping.

The entire armor assembly of *P. senegalus* is fairly complex. One way to explore this system is through decomposing the whole into smaller building blocks and relationships to decrease complexity. After identifying the system elements and relationships, they are then re-assembled (composing). During system recomposition, it is important to weight and restrict the system to simplify its complexity. In many cases, it is not important to completely mimic the whole system. Within the third step, the elements need to be put into order, a hierarchy. Then forth, through adding and removing elements and/or relationships the system can be adjusted or calibrated. Finally, by changing input information or other parameters the system can be deformed, for example to achieve gradients or differentiation. (see Goodman 1978)

Strategy of Decomposing the Biological System

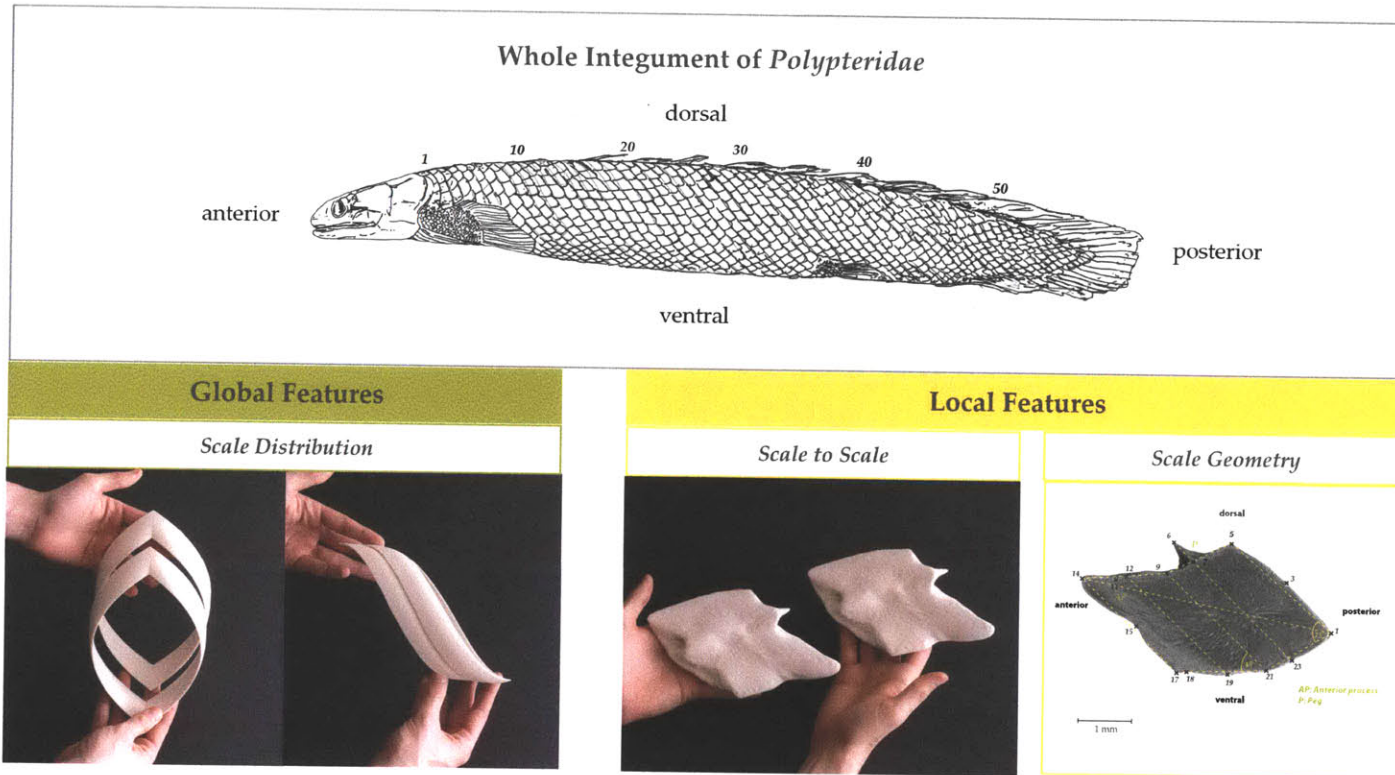


Figure 20: Diagram of the followed strategy of decomposing the complex biological design into one main global feature (scale distribution along the body) and two local features (scale-to-scale connections and single scale geometry)

Prototyping and Fabrication

To materialize the designs two different 3D printing techniques have been used. 3D rapid prototyping is a very fast way to produce a complex physical object from virtual 3D geometry. The first use of 3D printing techniques was the creation of scaled up physical prototypes of the real 3D scanned biological geometry derived from microcomputed tomography images. The goal of this procedure was to retrieve a physical understanding of the paraserial peg-and-socket connection, as well as the interserial sliding interface. The grayscale images from micro-computed tomography were converted into surface mesh geometry using the multi-platform, free open source software (FOSS) software 3D Slicer and was exported using the Stereolithography (STL) file format. This geometric surface information was imported into the commercially available CAD software called Rhinoceros 3D (McNeel) for cleaning the mesh geometry of noise and not necessary porosity. In the last step, the desired geometry was scaled up considering the maximum printable size given by the machine as well as structural requirements avoiding smaller wall thickness than 2 mm to reduce the risk for failures.

A 3D printing machine (ZPrinter® 310 Plus, ZCorporation, USA) was used for the initial fabrication process. The instrument spreads a commercially available plaster powder (ZP®131 powder, ZCorporation) of 89 micrometer thickness with a speed of 25 mm/h; next, a 2D pattern gets printed using ZCorp commercial available binder. This process was repeated layer by layer until the final prototypes were completed. The printed object rested within the powder bed for a minimum one hour to achieve its highest strength. Finally, the objects were saturated into a wax bath. The intention of this step was mainly to accomplish a less powdery surface finish, but also the strength and stiffness was slightly improved.

While the ZCorp plaster material is quite fragile, a different 3D printing technique was used for subsequent prototypes. The OBJET Connex500 3D printer can simultaneously combine multiple materials into a single prototype.

Methods

The OBJET Connex500 3D printer possesses a tray size of X = 500mm x Y = 400mm x Z = 200mm. 3D objects can be printed with a resolution of up to 1600 dpi in Z-axis (16-microns) and 600 dpi in X- and Y-axis (42-microns), while showing an accuracy of up to 0.1 to 0.3mm (0.004 to 0.01 inch). For the Objet multi-material 3D prints all designs have been generated using the parametric modeling environment (SOLIDWORKS®, Dassault Systèmes Solid-Works Corp., France). The scales, connective tissue and soft tissue were designed as separate parts and combined inside Solidworks into an assembly. To communicate with the 3D printing machine, all 3D parts within the assembly were exported into separate STL files. This collection of STL files was imported into OBJET Studio software which is able to identify assembled objects. For each imported STL part a specific materiality can then be applied within OBJET Studio.

During the 3D printing process the following materials were used. The ganoid scales have been simulated through a rigid material called Objet VeroWhite, while for the connective and soft tissue several materials have been tested. While the mixable, digital materials called Objet TangoBlack DM_9110 and Objet TangoBlack DM_9130 performed less flexibly than desired, the material system was changed to the much more flexible Objet TangoPlus DM9740. For all print jobs, the digital printing mode was used, performing with a resolution of 30 microns (0.001 inch).

Material Name	Hardness (Shore A)	Tensile Strength (MPa)	Elongation to break (%)
<i>TangoBlack DM_9130</i>	95	9	39
<i>TangoBlack DM_9110</i>	80	3	50
<i>TangoPlus DM_9740</i>	40	1	160

(ASTM D-2240) (ASTM D-412)

Table 1: Material properties used during multi-material prototyping

Results and Discussion

Introduction

In this chapter, experimental results are presented which quantify the maximum degree of body curvature and ranges of motion of an anesthetized *P. senegalus* in order to assess the anisotropic biomechanical capabilities of the fish. In the subsequent sections, the armor assembly is studied and mimicked at increasing complexity in order to understand the biomechanical mobility observed experimentally. Morphometric analysis was carried out on three-dimensional micro-computed tomography data of individual scales using landmark identification to quantify shape/form and was subsequently used in model design. MicroCT data was reverse engineered to generate increasingly complex, larger size scale bio-inspired physical models (prototypes) of the armor units and armor assembly using 3D printing fabrication methods. Last, the geometric and functional features were captured within a parametric design model. A simplified monolithic scale assembly as well as a multi-material, integrating the rigid unit geometry with flexible connections, were fabricated. Both physical prototypes show very similar anisotropic mechanical behavior compared to their biological model, the *P. senegalus* integument.

Maximum Body Curvatures of *P. senegalus*

An anesthetized *P. senegalus* was manually manipulated to quantify ranges of motion and maximum radii of curvatures of the entire fish body in different directions (Figure 21). The measured radii have been related to the body length excluding the tail fin.

Maximum radii of curvature of ~17 mm (inner) and ~31 mm (outer) were measured in the XY plane. Maximum radii of curvature of ~59 mm (inner) and ~87 mm (outer) were measured in the XZ plane. These measurements are consistent with those reported in the literature (Gemballa and Bartsch 2002), the tested *P. senegalus* can achieve body curvature radii of around 8 % of its body length.

Results and Discussion

Reference Length

Experiment: Juha Song
Photography: Steffen Reichert

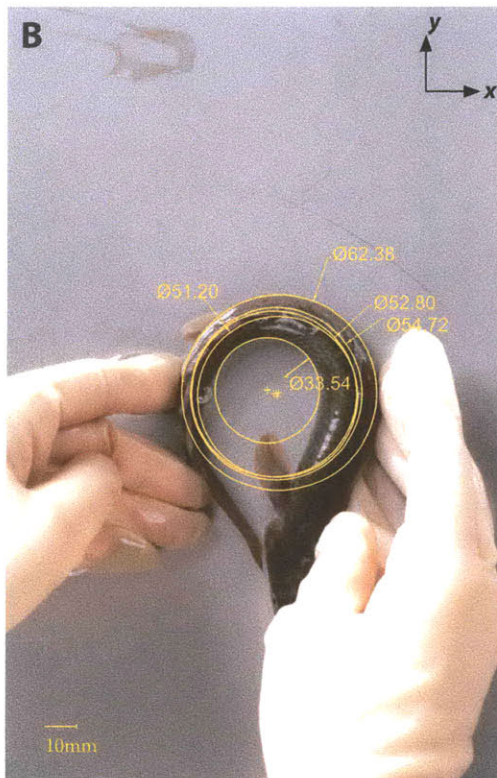


Total Length: ~219 mm

Body Length: ~202 mm (L = 100%)

Weight: ~34 g

XY-Curvature



Inner radius: ~17mm (8% of L)
Outer radius: ~31mm (15% of L)
Central radius: ~26+0.9mm (13% of L)
Inner radius = compression.
Outer radius = tension

XY-Curvature



Inner radius: ~19mm (9% of L)
Outer radius: ~30mm (14% of L)
Central radius: ~31+2.8mm (15% of L)
Inner radius = compression.
Outer radius = tension

Figure 21: (Captions see following page)

Results and Discussion

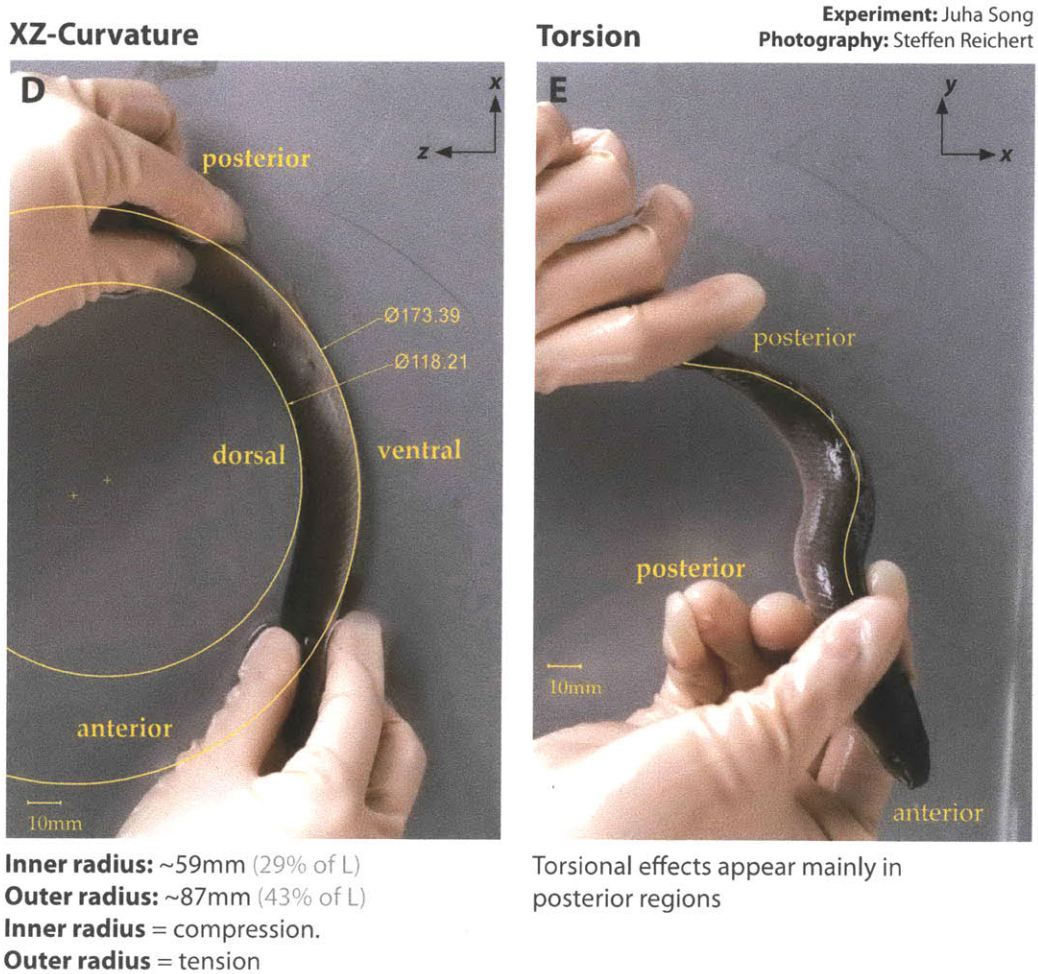


Figure 21: (A) *P. senegalus* in resting position, showing a total length of ~219mm. Excluding the tail fin a body length (L) of ~202mm results. (B-C) Within the XY-plane the *P. senegalus* specimen showed a constant body curvature of ~8%. (D) In the XZ-plane a body curvature of ~29% was measured. (E) Even torsional motion was captured.

It is fascinating how *P. senegalus* combines extreme body curvatures while still possessing a very protective scale integument assembled out of highly mineralized, rigid scales. Gemballa and Bartsch claim that the ganoid integument of *Polypteridae* is not a limiting factor of the flexibility of the fish. This suggests that the interlocking scales are designed to allow the specific flexibility (functionality) which is needed by the fish.

Results and Discussion

Landmark Identification

To analyze geometrical differences in shape of the scales along its body, a 3D morphometric analysis was employed (see Background Chapter). The geometry of *P. senegalus* scales was decomposed through the position of landmark points (Figure 22). In total, 26 landmarks were identified and classified as shown in Table 1. *P. senegalus* scales possess the motion constraining peg-and-socket joint geometry. To identify the specific articulation, the peg-and-socket geometry has been segmented to identify the allowed range of motion between the peg and socket.

Table of Landmark Locations

Landmark	Type	Description
L(1)	2	Tip exterior, most posterior point
L(2)	2	Tip interior, most posterior point
L(3)	3	Exterior point, dorsal
L(4)	3	Interior point, dorsal
L(5)	1	Most dorsal point
L(6)	1	Tip of peg, most dorsal point
L(7)	2	Exterior junction peg/scale
L(8)	2	Dorsal angle point, interior
L(9)	2	Dorsal angle point, exterior
L(10)	3	Interior point, dorsal
L(11)	2	Most exterior point, dorsal
L(12)	3	Midpoint, dorsal
L(13)	3	Interior point, dorsal
L(14)	1	Most anterior point (anterior process)
L(15)	2	Valley, ventral point
L(16)	2	Ventral point
L(17)	1	Most ventral point
L(18)	2	Ventral point
L(19)	3	Ventral point, exterior
L(20)	3	Ventral point, interior
L(21)	2	Ventral angle point, interior
L(22)	2	Ventral angle point, exterior
L(23)	2	Interior valley, entrance to socket
L(24)	2	Anterior point in peg and socket axis
L(25)	1	Center of socket
L(26)	3	Interior point at socket entrance

Table 2: 26 landmarks were identified, classified and described.

Results and Discussion

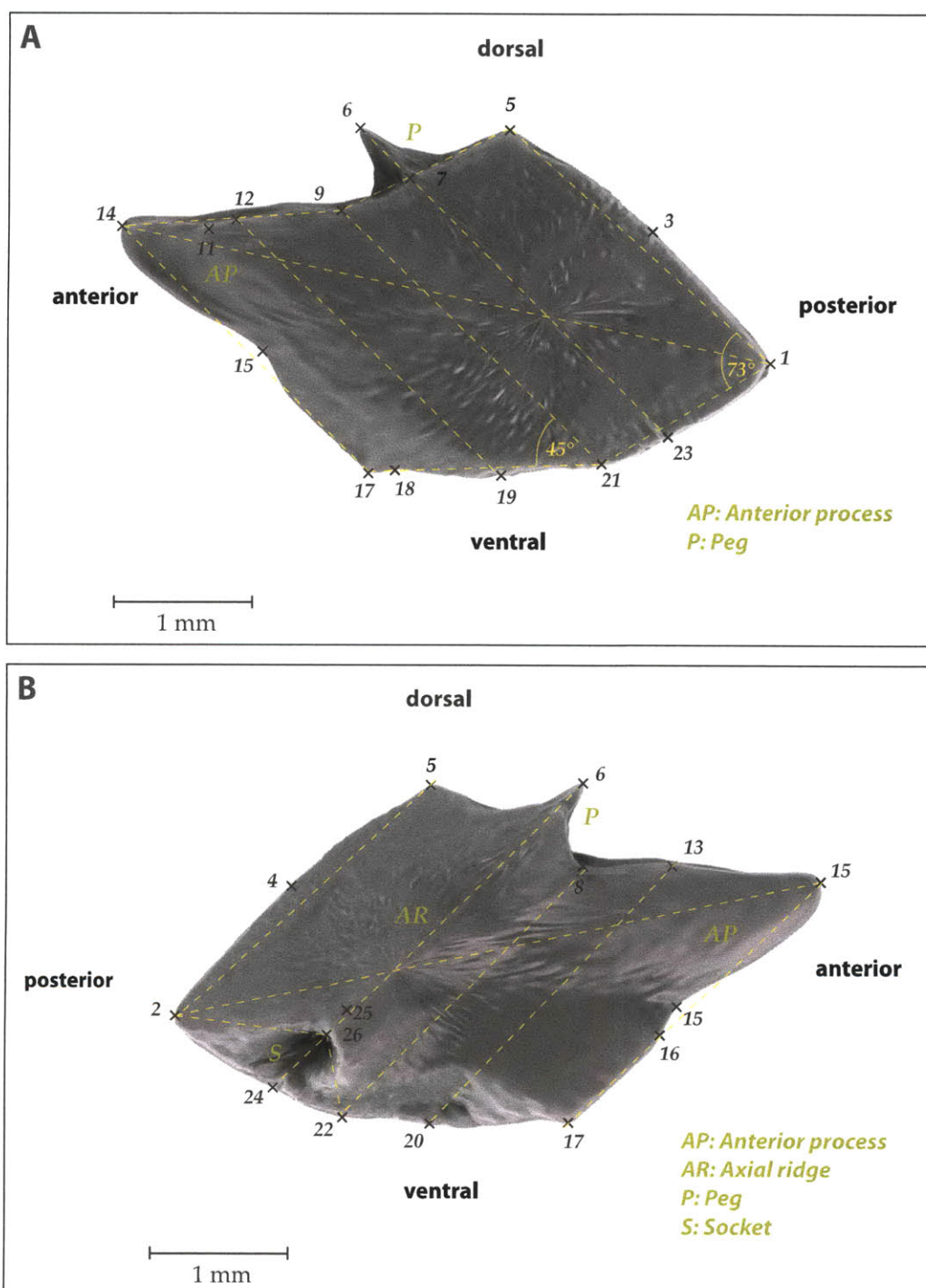


Figure 22: 26 Identified landmarks on an individual scale of *P. senegalus*. Microcomputed tomography was used to measure three dimensional structural data of the scales. This micro-computed tomography was used to generate precise 3D information of the biological forms. (A) Exterior view, (B) interior view

Results and Discussion

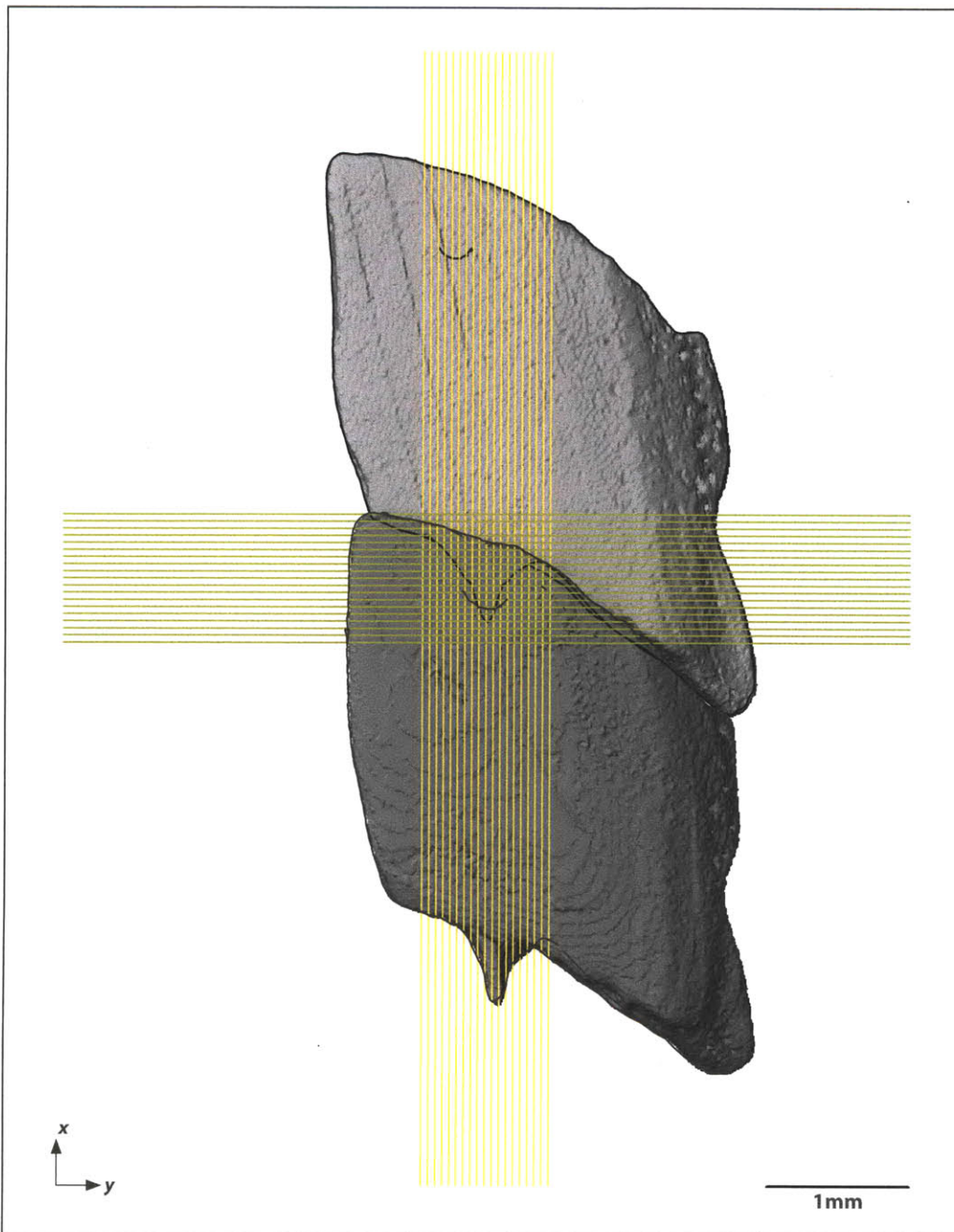


Figure 23: An automated sectioning script was developed, exploring the geometry of the interlocking peg-and-socket geometry between two scales of *P. senegalus*.

Results and Discussion

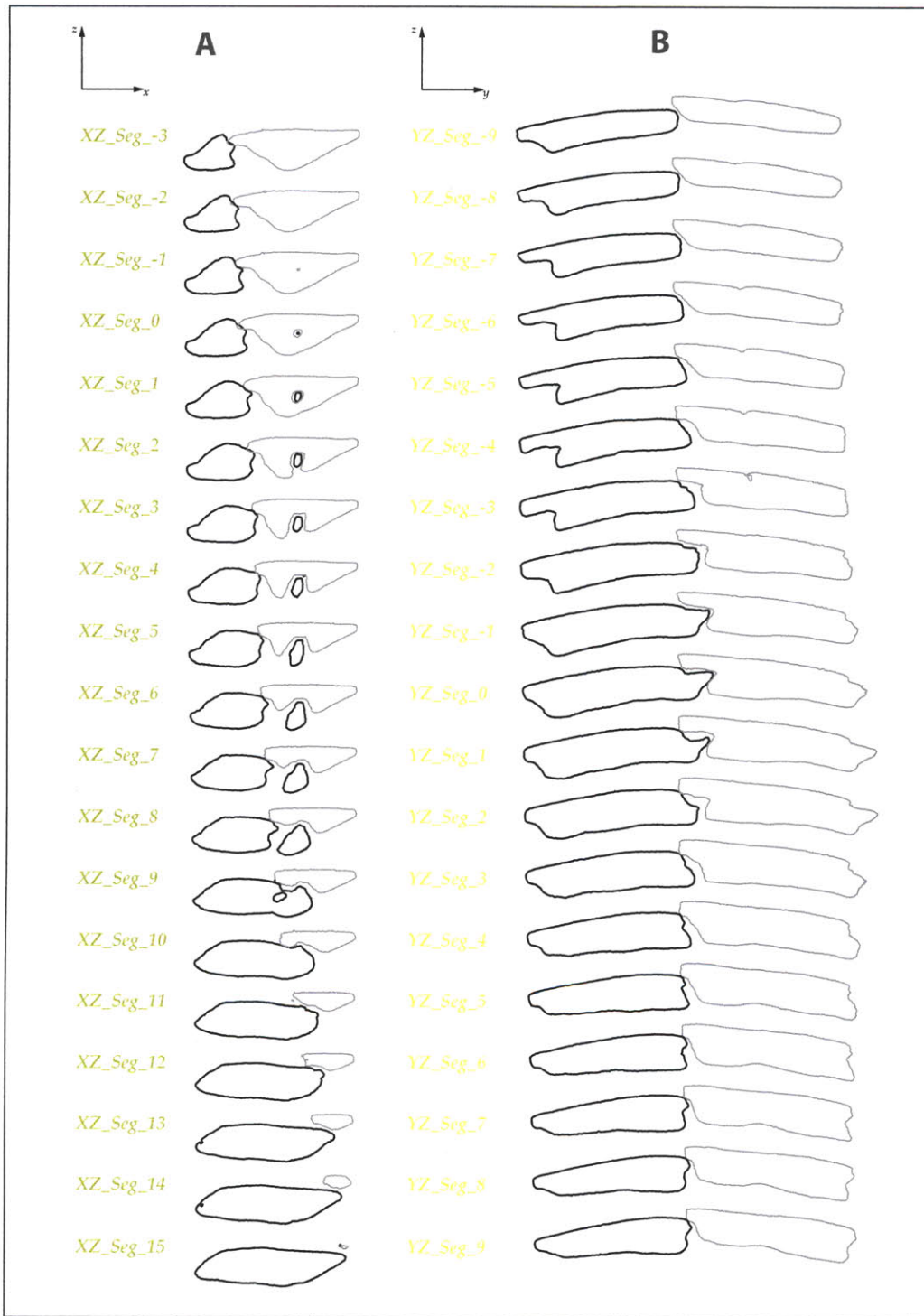


Figure 24: The resulting geometric outlines of the peg-and-socket geometry. (A) The sections in X-direction showed the free space between peg and socket. (B) In Y-direction, the scales provide a protective layer with constant thickness including the joint geometry.

Results and Discussion

Global Symmetric Helical Rings

As mentioned in the background chapter, the scales of *P. senegalus* are arranged in a closed mirrored helix configuration where peg-and-socket joints connect scales parallel to the helix rows (paraserial direction) and scales overlap laterally between helix rows (interserial direction, Figure 7 and 22). This anisotropic assembly raises a number of interesting questions:

1. Why is the armor of the fish body not constructed out of solid (monolithic) symmetric helical rings instead of being subdivided into scales, with the much more complex organic-reinforced peg-and-socket joints?
2. Does the global mirrored helix geometric articulation itself allow certain degrees of freedom and if yes, what is the range of motion?

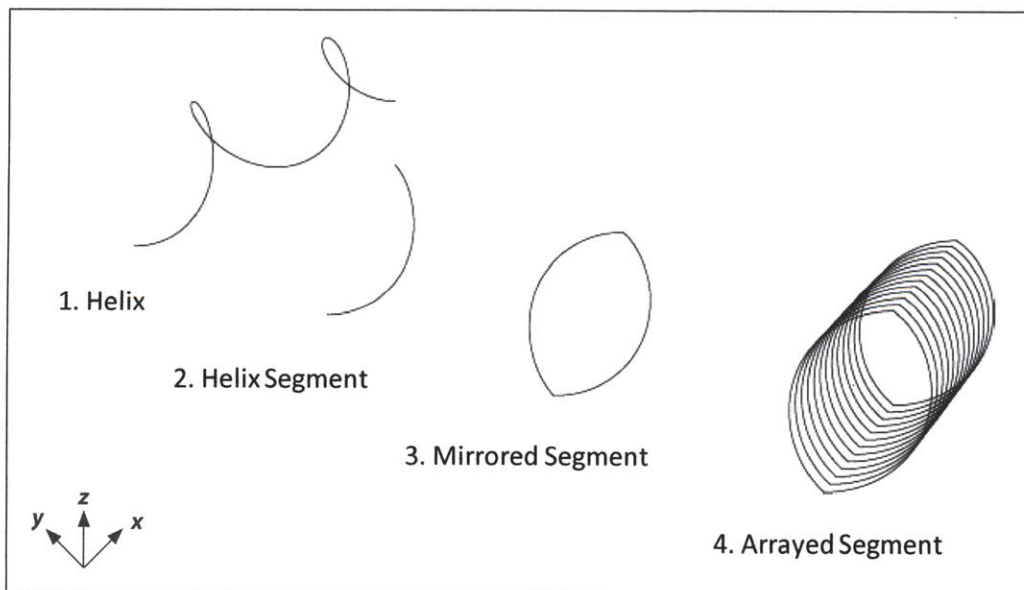


Figure 25: The helical, global distribution of scales for *P. senegalus* was simulated by helix segments. Through mirroring by the XZ-plane, closed symmetrical rings got generated. Last, these rings were arrayed along the Y-Axis to mimic the helical distribution of the fish armor.

Results and Discussion

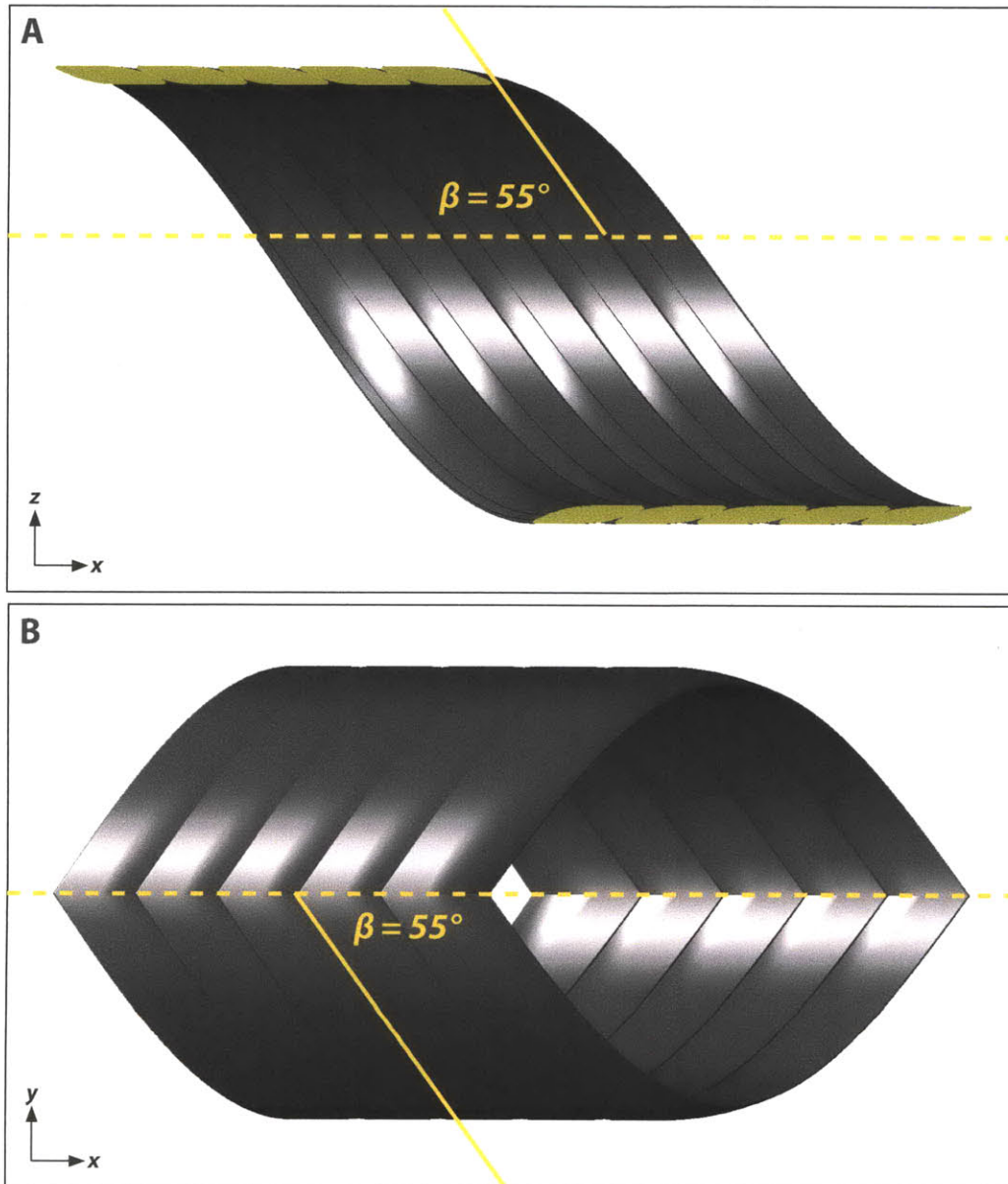


Figure 26: The virtual 3D NURBS model of global, symmetric helical rings in (A) section view and (B) top view.

Results and Discussion

To answer these questions, a digital model of monolithic symmetric mirrored helical rings was created at a 55° helix angle as measured for *P. senegalus* (Figure 26). This digital model was used to fabricate two symmetric helical rings using ZCorp 3D printing technology (Figure 27). The physical prototype does not show any degrees of freedom. The two identical rings with a symmetric helical shape fit perfectly onto each other showing a contact curve along the ring. This results that this global strategy of arranging the scales does not primarily add any freedom to the overall system, which implies that the overall flexibility can be reduced to the two different scale-to-scale connections (parallel to the helical rows and lateral to the helical rows).

As a result, the physical prototype does not show any degrees of freedom. The two identical rings with a symmetric helical shape fit perfectly onto each other showing a contact curve along on the ring. This concludes that this global strategy of arranging the scales does not primarily add any freedom to the overall system, which implies that the overall flexibility can be reduced to the two different scale-to-scale connections.

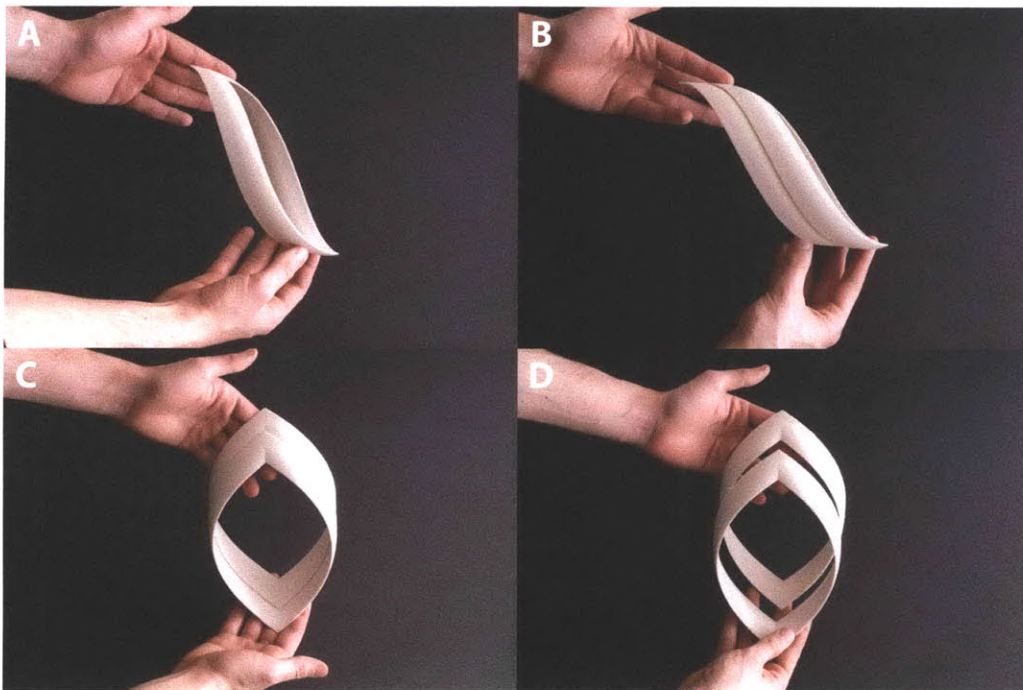


Figure 27: 3D printed prototype of the monolithic scale row. (A) One single symmetric helical ring. (B) Two true scale rows in assembled configuration. Within the assembly the rings interlock perfectly and constrain all degrees of freedom.

Results and Discussion

Unitizing Scanned Scale Geometry

The following section shows two strategies to reverse engineer the complex scale geometry of *P. senegalus* scales. The 3D mesh geometry generated by this process may serve as source for further investigations. First, the scale geometry was reconstructed using a linear sectioning technique. The second radial sectioning technique showed improvements in simplicity and automation.

Since the geometry of the scales, including the peg-and-socket joints, varies throughout the fish body, for simplification in a bio-inspired model scale assembly, a single unitized scale was generated and utilized as a representation of a typical scale, thereby removing differentiation phenomena. Hence, microCT data from two neighboring fish scales central to the fish body were employed for unitizing the scale geometry. In this strategy of modularization, the geometry of these two neighboring scales were merged into a single design, the unitized scale, which was subsequently used for creating the assembly prototype which is expected to closely approximate the real armor of *P. senegalus*. The process of 'unitizing' was started by superimposing both scale meshes. Next, the meshes were divided into two halves. (Figure 23) Focusing only on the neighboring peg-and-socket sections the other peg-and-socket geometry from each scale was erased. One peg and one socket half each from one of the neighboring scales remained and served as basis for the following two NURBS conversion strategies.

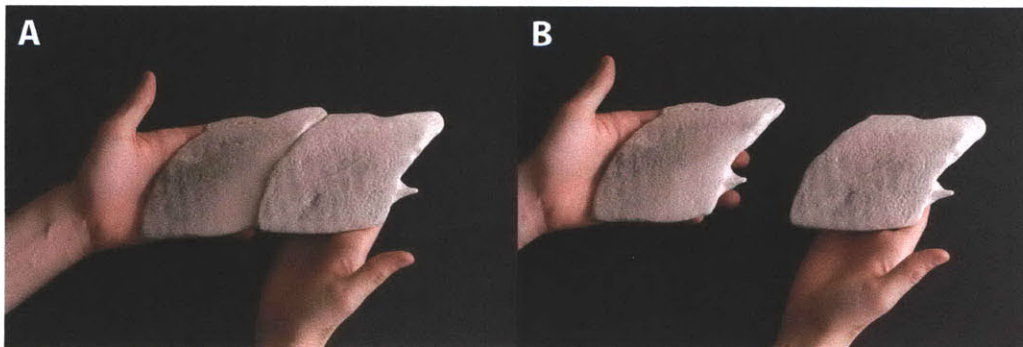


Figure 28: Microcomputed tomography scanning was used to generate 3D mesh information of *P. senegalus* fish scales. The 3D mesh geometry information was directly used for 3D printed prototypes (1:37.5)

Results and Discussion

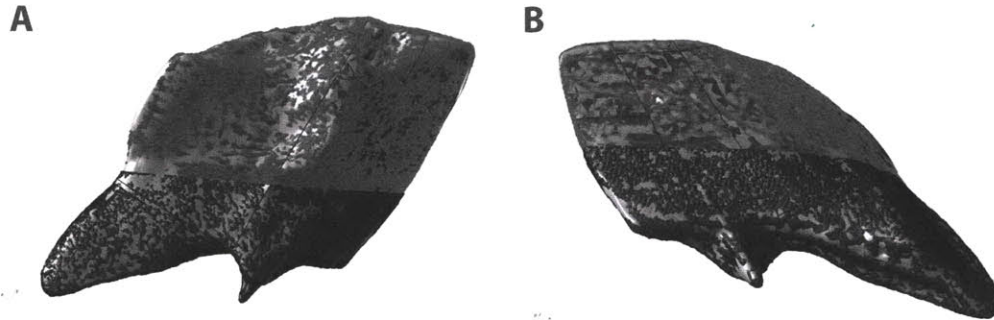


Figure 29: Two neighboring scales have been separated and reassembled into one “unitized” scale geometry that can be assembled to bigger arrangements.

Linear Sections

The first attempt was focused on using linear, parallel section curves to generate a lofted closed solid geometry. To generate a closed polysurface, it was necessary to split the geometry into several surface regions. A complicated surface patchwork is the result to achieve a solidified geometry.

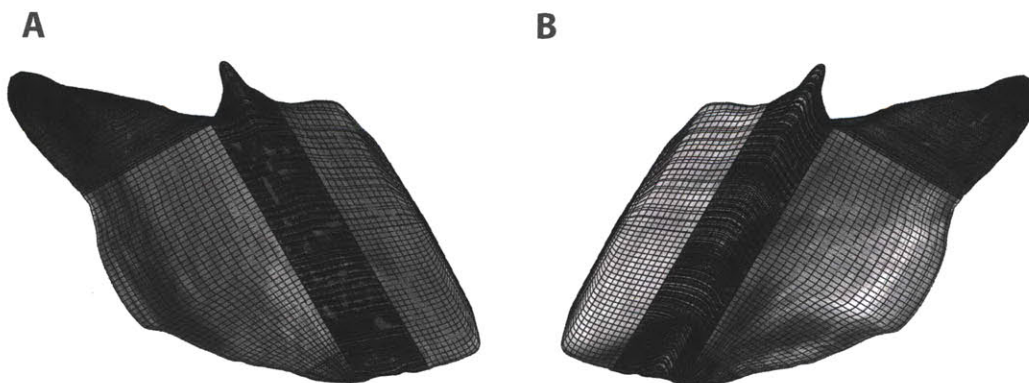


Figure 30: Reverse engineered scales using a linear sectioning technique. Resulting geometry consists out of several NURBS surfaces that have been joined into solid geometry.

Results and Discussion

Radial Sections

The second approach is based on a radial sectioning of the two scale geometries around a single center point (C). The center point was derived as the intersection point between the peg-and-socket axis and the axis between the most anterior and most posterior tip. Following this strategy of placing, the center point no undercuts will appear. Then, through projection, section curves can be generated radially onto the mesh geometry. The result is a circular array of open curves that can be lofted and joined into one single NURBS surface. This is a simplified way of reverse engineering the complex fish scale geometry can be fully automated. Very detailed meshes based fish scale geometries can be converted in smooth surface. This is of high value for future investigations in the differentiation of the scales.

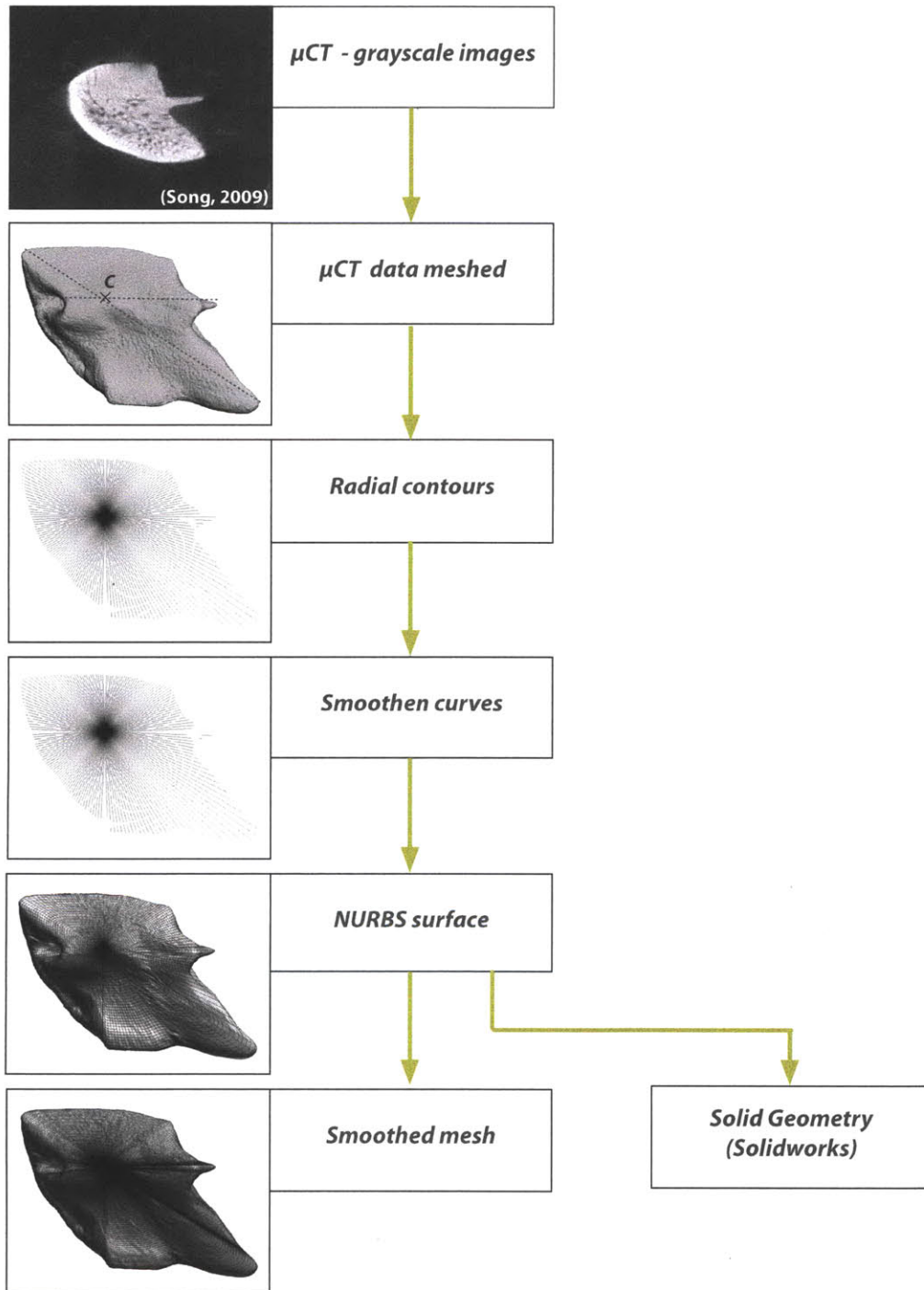


Figure 31: Using a radial sectioning technique, it was possible to represent the complex geometry of *P. senegalus* scales through a single lofted NURBS surface.

Results and Discussion

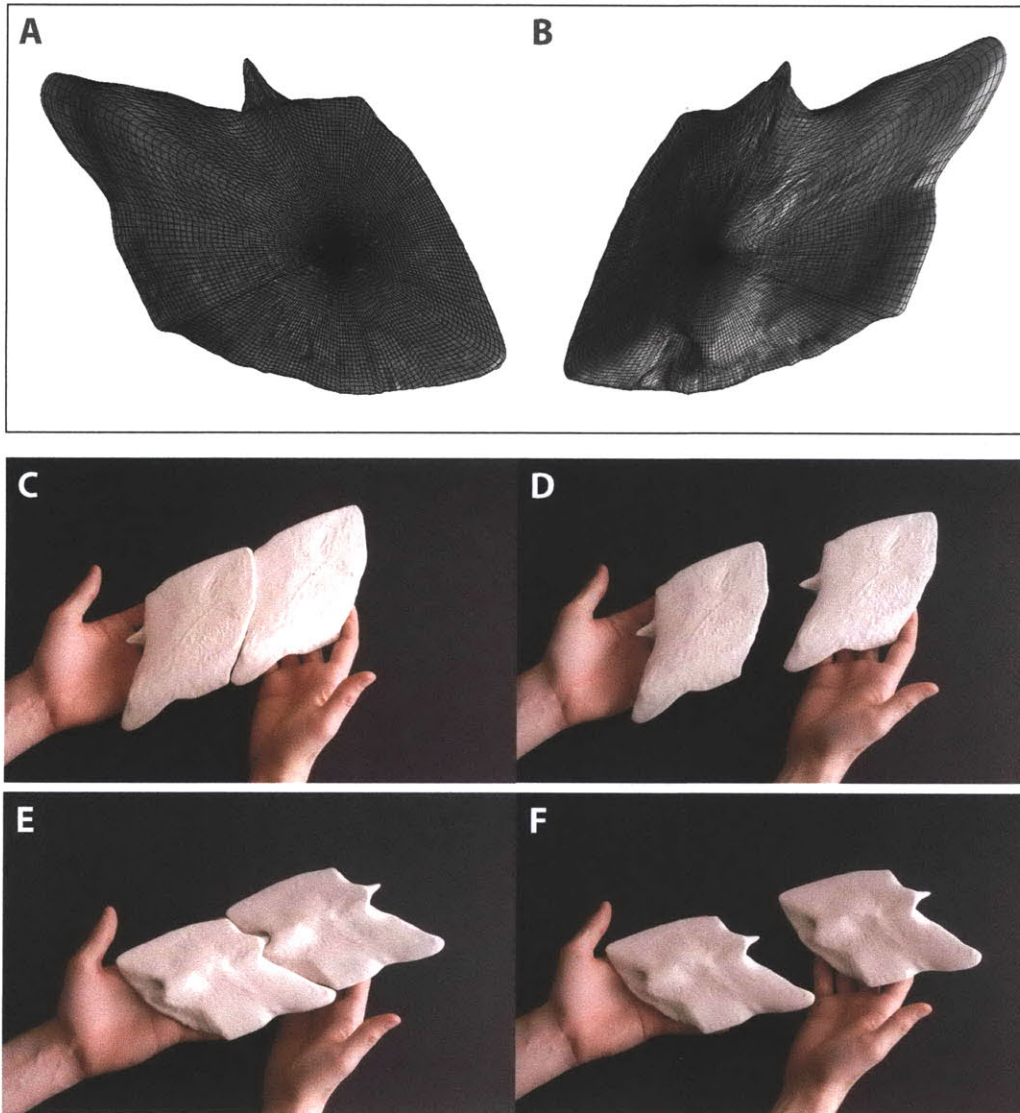


Figure 32: Detailed images of reversed engineered, 'unitized' *Polypterus senegalus* scales, from (A) exterior and (B) interior perspective. Images (C-F) show 3D printed prototypes using ZCorp 3D printing technology. (1: 40)

Results and Discussion

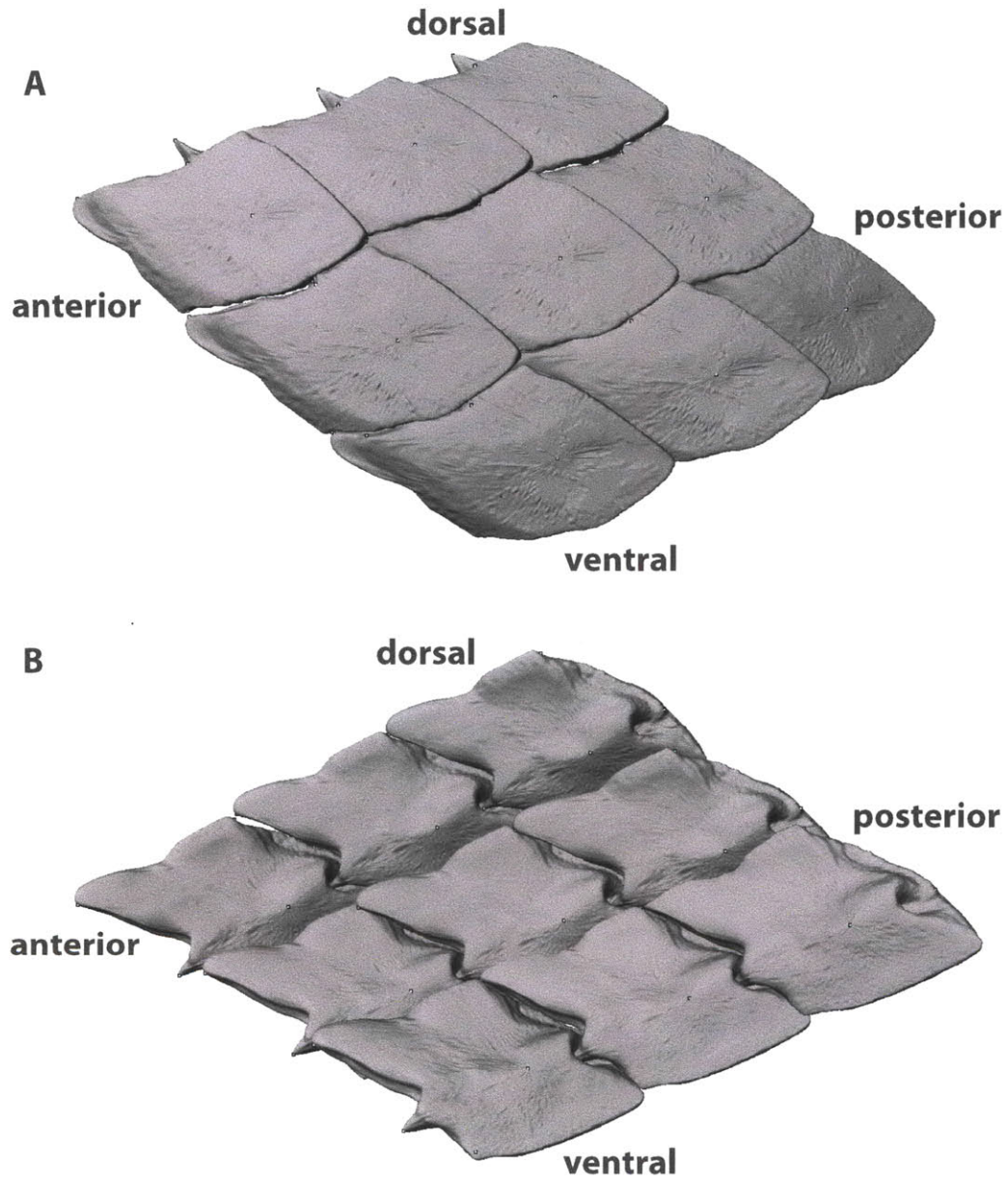


Figure 33: Virtual 'Unitized' scale assembly from (A) exterior and (B) interior view.

Results and Discussion

The reverse engineering process and physical prototyping helped to get a detailed understanding of the allowed flexibility within the paraserial peg-and-socket joint as well as along the interserial sliding faces. In paraserial direction considering the tight Shapery's fiber tissue only two rotational degrees of freedom are possible. The mating surfaces constrain the third rotational degree of freedom. Due to peg-and-socket joint all transitional motion are completely restricted. In the paraserial direction, more flexibility has been explored. Two rotational as well as two translational motions seem to appear during the locomotion of *P. senegalus*.

The two strategies of reverse engineering scale designs closely related to the scanned fish scale geometry was not continued because of the following reasons.

Advantages

On the one hand being very close to the geometry of the biological system is highly advantageous, but on the other hand it can also be highly disadvantageous in terms of decomposing the system and representing smaller aspects in geometric terms. For this reason a more simplified design approach might be more insightful and will make the main biological principles more understandable.

Disadvantages

The complex geometry of the reproduced, 'unitized' scales will make it very difficult to manipulate the geometry. Even though deformation procedures can probably fulfill the desired geometric changes, but compared to a parametric design model it will be much more difficult to control. Even though, none of the presented strategy of geometry data was proceeded, it was still a very important part of the learning process of understanding the specific biological shape. Since design investigations are only very seldomly similar, a process of trial and error is necessary to find the best technique or method for a specific problem.

Results and Discussion

Simplified Anisotropic Scale Assembly Design Model

In the following section a highly simplified scale assembly design model is introduced. This abstracted design explores, extracts and presents the main motions of the scale integument; first in the scale-to-scale relationship and then the scale assembly. The scale design was generated as a parametric model. Parametric modelling allows for the generation of a hierarchical associative design model. Within this logically defined model, parameters can be modified to adjust a design according to subsequent insights.

“Whenever two solid bodies are in contact we may treat the contact zone as a joint.”
(Gans 1980)

All motions between two objects can be described by six degrees of freedom. These degrees of freedom can be separated into 3 translational (travel along an axis) and 3 rotational (motion around an axis) motions. (Gans 1980) In natural as well as in synthetic systems, the more degrees of freedom (liberty) a joint possesses the more possibilities of motion it allows. (Gans 1980). But also the more possibilities of motions a system allows, the more complicated it is to describe or control. (Gans 1980). Therefore, the fewer degrees of freedom allowed within a joint, the easier is its description. (Gans 1980).

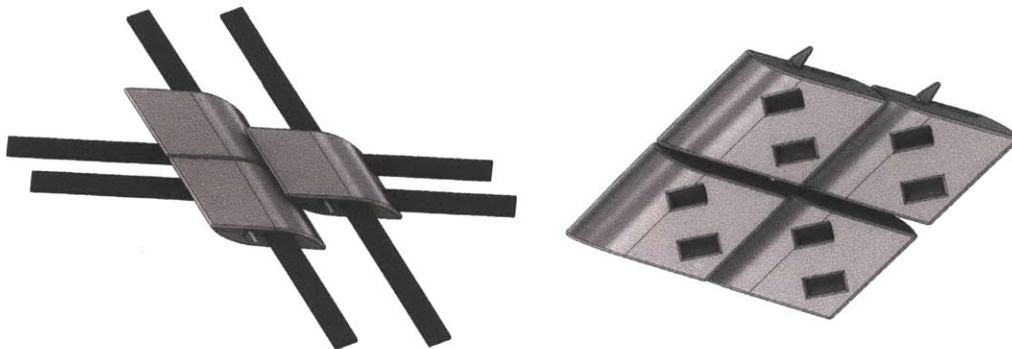


Figure 34: Simplified scale design that was assembled with rubber bands.

Results and Discussion

Paraserial Peg and Socket Joint

As presented in the background chapter, the scales of *P. senegalus* possess a motion constraining peg-and-socket joint in paraserial direction. On the dorsal surface of each scale a peg protrusion is visible and fits into socket geometry in ventral region. This interlocking, geometric feature is of critical importance in determining the biomechanical behavior of the whole armor assembly because it highly constrains the degrees of freedom and ranges of motion between each scale-to-scale connection.

In the highly simplified scale design, the peg geometry is mimicked through a geometry similar to tetrahedra. To the outer direction of the scale, the peg possesses a rounded surface and thickens up to the inside of the geometry. The corresponding socket design is very similar but concavely designed and is constructed slightly larger. These angles (α , β) (Figure 36 and 36) allow a precisely controllable range of rotational motion around the X-axis. The slightly bigger peg shows free space underneath the peg and in combination with the slightly tapered profile of the dorsal and ventral surface of the scale, ranges of rotational motion is allowed around the Y-axis (Figure 35 and 36). The rotational degree of freedom is limited by the facing dorsal and ventral surface and two translational degrees of freedom around the Y- and Z-axis are restricted by the peg protrusion. Additionally, the last degree of freedom in the biological system is highly constrained by the paraserial collagenous fiber connection (Sharpey's fibers) (Gemballa and Bartsch 2002). This fiber connection is simulated in this prototype through a rubber band connecting the scales along the paraserial row axis.

Interserial Overlapping Interface

The interserial interface of neighboring scale rows allows large degrees of freedom and accordingly, also a high degree of motion. Each scale row is overlapped by the posterior region of the anterior, neighboring scale row. The interserial overlap connection allows four different degrees of freedom presented in

Results and Discussion

Figure 35 and 37 They can be divided into two translational and two rotational motions. The translational motion along the Y-axis is the most prominent motion (Figure 35 and 37) . It allows compression and extension of the scale armor on the fish and can be explored most greatly at the most lateral fish scales. In these regions, a scale overlap ranging from 42% up to 140% has been measured in literature. (Gemballa and Bartsch 2002) (Note that these measurements include both overlaps at the same time, which means if the anterior neighboring scale overlaps 70% and the posterior 70%, a total overlap of around 140% can be measured.) The second most important degree of freedom is the rotational motion around the X-axis (Figure 35 and 37). This degree of freedom allows torsional motion within a scale row.

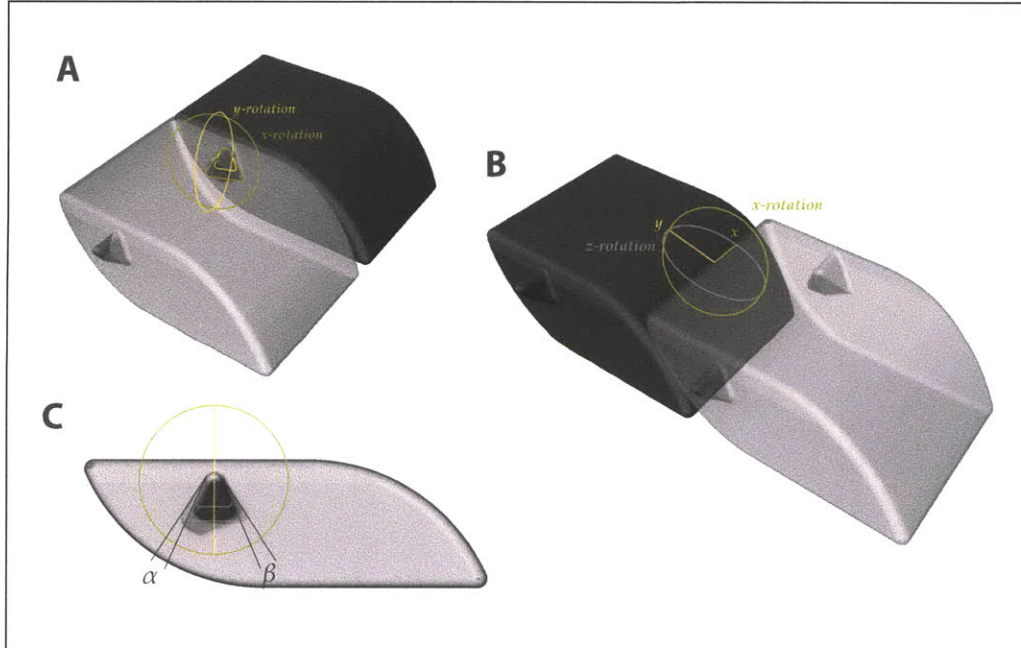


Figure 35: The simplified scale design was designed to allow two rotational degrees of freedom at the (A) paraserial peg-and-socket connection and (B) at the interserial sliding interface. (C) The peg and socket within this design allows two discrete ranges of motion (α , β).

Results and Discussion

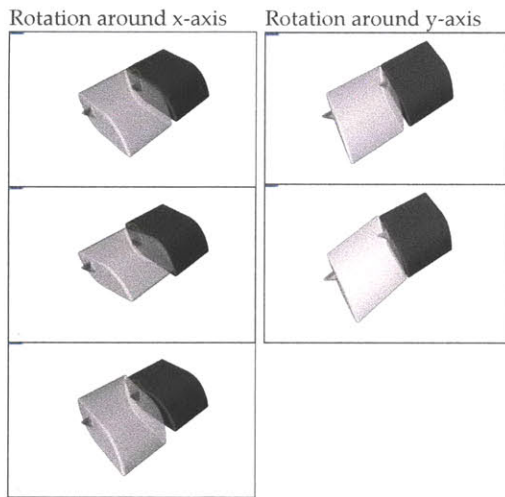


Figure 36: Within the assembly, the scales perform in paraserial direction in two rotational degrees of freedom. Rotational motion around the X-axis is limited by the angled free space between the peg and the bigger socket.

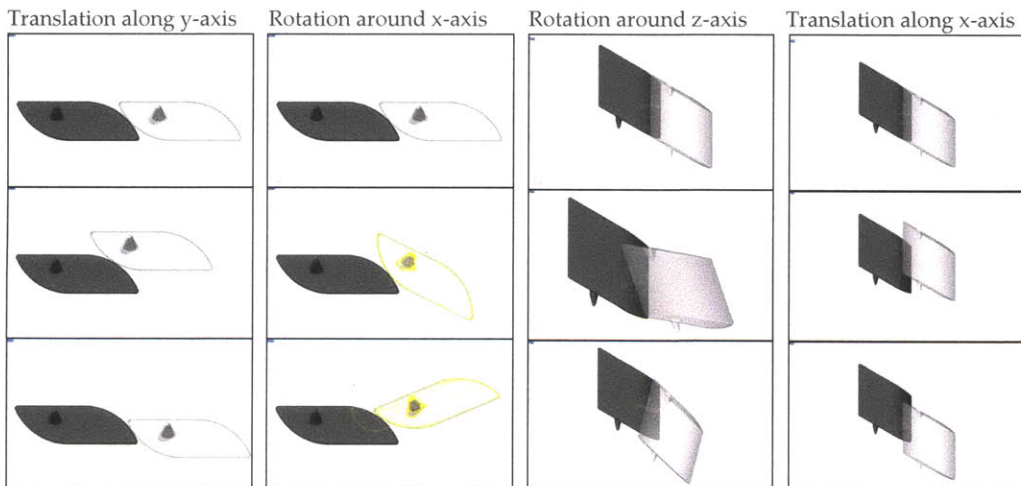


Figure 37: In interserial direction, the overlapping interface allows much more flexibility. Four different degrees of freedom were explored, two rotational motions (around X- and Z-axis) and two translational motions (along the X- and Y-axis).

Results and Discussion

Simplified Scale Assembly

The goal of this simplified scale integument is to explore the controlled scale-to-scale behavior within an assembly. The fiber connections in the paraserial but also in the interserial direction are simulated through rubber bands linking together scales in the paraserial as well as the interserial direction. In the paraserial direction the rubber band is fed through a straight extruded cut within the scale body oriented parallel to the peg direction. In the interserial direction, rubber bands connect scales diagonally with each other using rotational cut conduit.

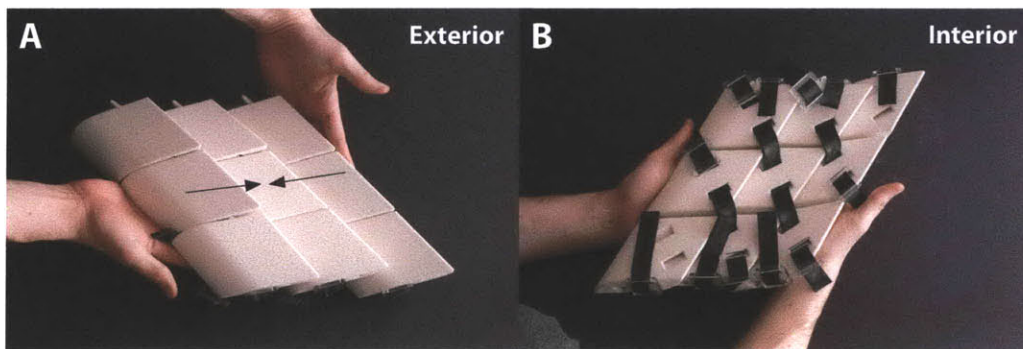


Figure 38: Simplified scale assembly in compression state.

Compression:

The assembly allows compressive behavior (Figure 38A-B). In this state the row of scales tries to overlap as far as possible. The range of motion is limited to the flexibility and the interserial length of the rubber bands connecting the scale rows with each other. The paraserial peg and socket connection does not perform any motion. This movement can be explored at the inner radius of the fish armor curvature.

Results and Discussion

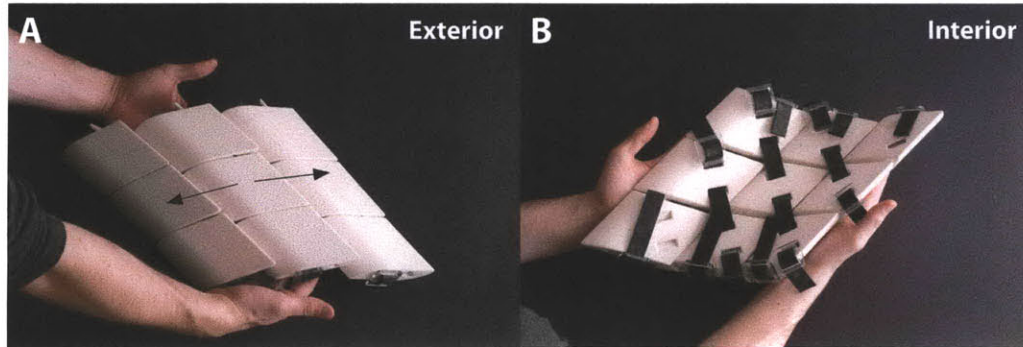


Figure 39: Simplified scale assembly in tension state.

Tension:

The tensional state (Figure 39A-B) is the inverse of the state of compression. Here, the scale rows slide away from each other trying to achieve the largest surface area. As well as in the compression state the motion is limited by the length and flexibility of the rubber bands and the paraserial peg-and-socket connection is not affected. This movement can be compared to the outer radius of the fish armor curvature.

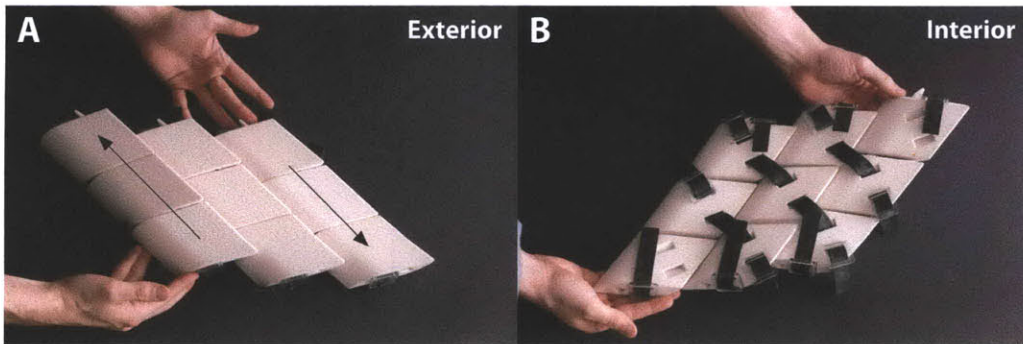


Figure 40: Simplified scale assembly in shear state.

Shear:

As shear (Figure 40A-B), the sliding motion parallel to the scale rows is described. This motion shows anisotropic behavior because according to the diagonal direction one motion shows more tensional resistance of the rubber band than the other direction. In the other direction the movement results in bending of the rubber band. Also here, the peg-and-socket motion is not affected. On the fish armor, this motion is important to produce vertical curvature.

Results and Discussion

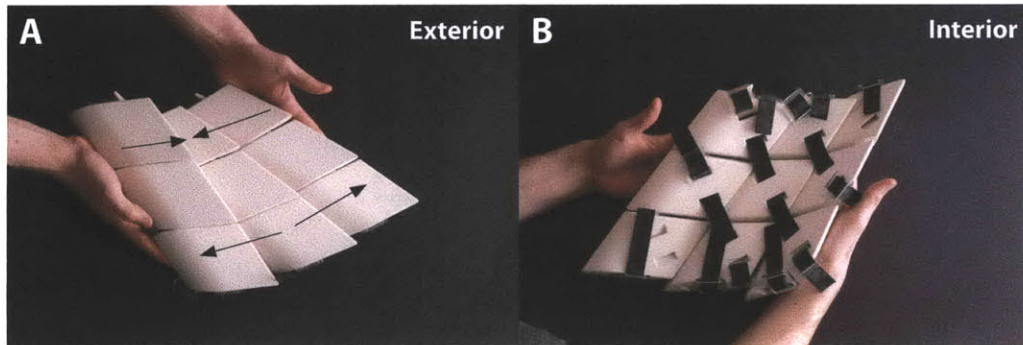


Figure 41: Simplified scale assembly in splay state.

Splay:

Splay (Figure 41A-B) can be described as tilting the scale rows at an angle. In this scale the rows' axes leave their parallel orientation. This motion must be similar to the shear responsible for the vertical curvature on the fish body. Depending on the shape of the scales and ranges on motion, some ranges of motion between the peg and socket joint need to be allowed to close gaps.

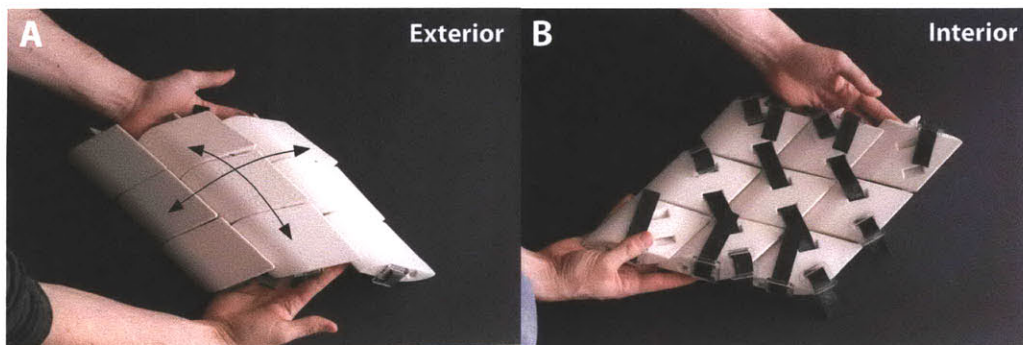


Figure 42: Simplified scale assembly in double curvature state.

Double curvature:

Double curvature (Figure 42A-B) bends the integument within both directions. In this case, motion can be observed at the paraserial as well as at interserial connection.

Results and Discussion

In this prototype, the rubber bands show very compliant behavior. Given the experimental observations of *P. senegalus* it is unlikely that the true organic is similarly compliant. Especially in the paraserial direction the rubber bands show no restricting resistance which stands in contrast to the Sharpey's fibers appearing in the biological system.

The highly simplified design was focused on exploring the main degrees of freedom within the two different scale connections as well as exploring the possibilities of customizing the design to prospective functional needs.

Results and Discussion

Multi-Material Prototyping of the Whole Integument Including Connective Tissue

While the previous prototype used a very abstracted and simplified design, for the next physical prototype a parametric design model was created incorporating more geometric morphological details of the fish scales as well as a much closer representation of the biological connective tissue. As a fabrication technique the Objet 3D-Multi-Material-Printing Technology was incorporated. The goal of this prototype was to achieve a much closer comparison to the biological inspiration focusing the exploration particularly on the connective tissue.

The landmark locations served as a starting point to define the geometry (Figure 44). Defining landmarks helped to identify the different geometric features in a complex geometry.

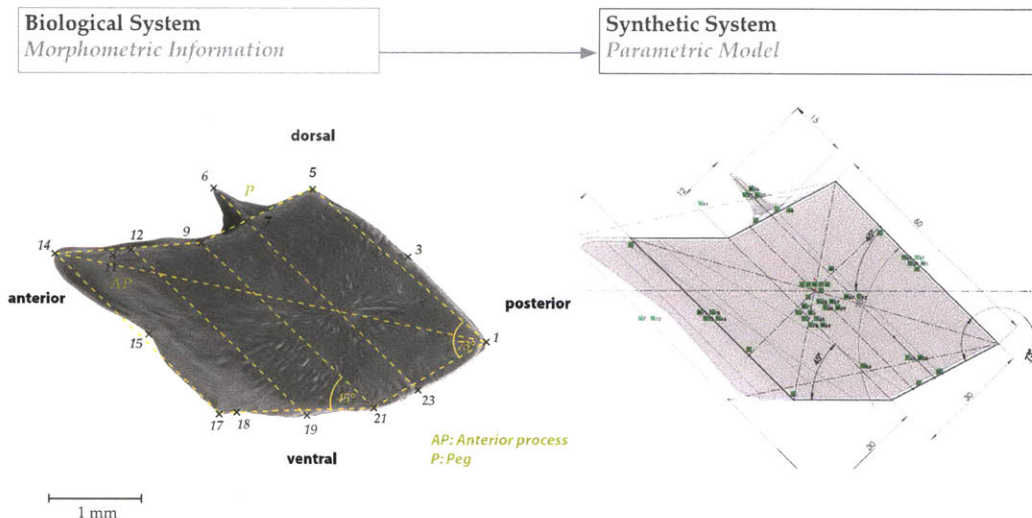


Figure 43: In the final prototype, morphometric information served as a basis for the parametric description.

Results and Discussion

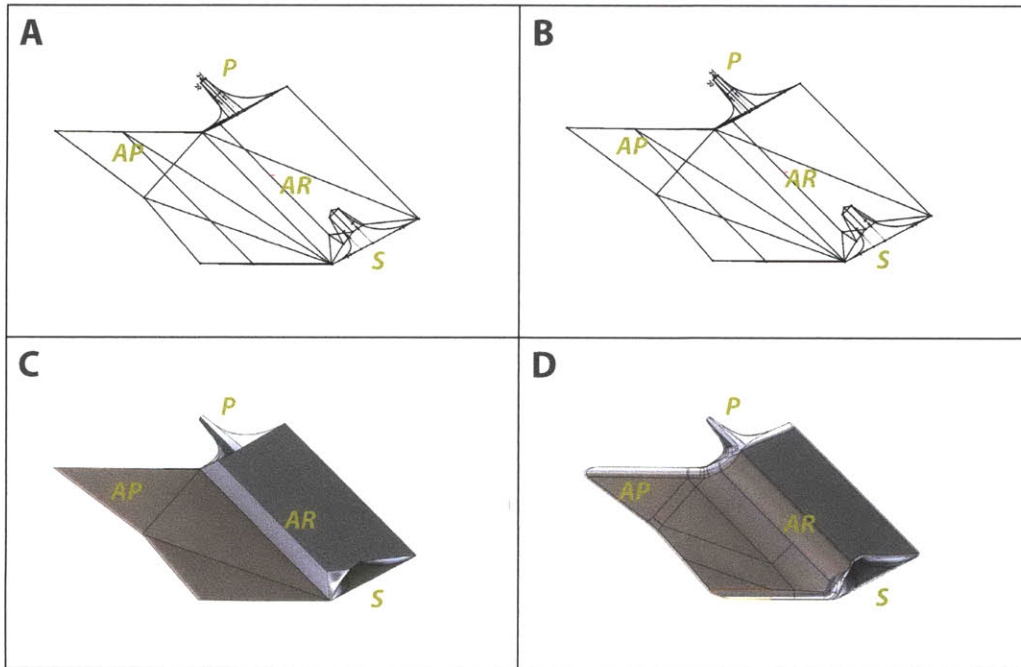


Figure 44:

(A) The first step of designing a parametric model of the rhomboidal scales by Polypteridae was to define the main geometric features within a two dimensional sketch. The design was highly influenced by the proportions derived from morphometric measurements of the fish scales.

(B) In the next step, out of the two dimensional sketch a three dimensional sketch was created. This 3 dimensional sketch served as the main geometric framework for the scale design, incorporating many geometric morphological details, e.g. axial ridge, anterior process, and anterior margin, as well as the angled dorsal and ventral surface.

(C) In the third step, the three dimensional sketch served as a kind of three dimensional scaffolding to represent the geometry through surfaces. A closed polysurface results and can be converted in solid geometry.

(D) Finally, sharp edges have been filleted not only to visually match the biological idol, in fact mainly to avoid stress concentrations and cracks at the edges.

Results and Discussion

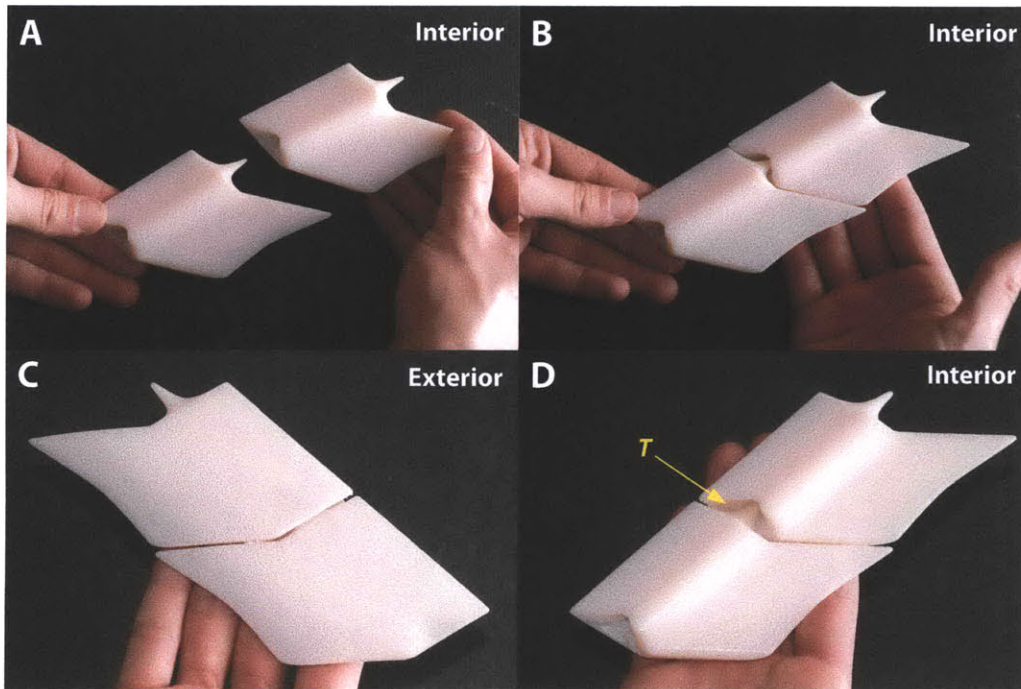


Figure 45: The scale geometry was 3D printed using OBJET multi-material printing technology. (A) Two single scales fit perfectly (B) along paraserial axis. (C) A softer material was included in the second prototype which simulated the (D) collagenous fibers (T) between the peg-and-socket joint.

Compared to the simplified model, the peg-and-socket joint geometry was greatly improved. The new more filleted design allows a much better stress distribution. As a whole squamation, the scales were assembled to a linear two dimensional pattern. Within the peg and socket, a Boolean extrusion part was used to simulate the longitudinal fiber connections (Sharpey's fibers). The stratum compactum was mimicked through a thin layer, spanning from axial ridge to axial ridge and allowing necessary freedom for motion. The connective stratum compactum was supported by a much thicker and much softer material block to simulate the internal soft tissue of the fish.

The physical multi-material prototypes show very similar mechanical behavior compared to the previous simplified scale design. Using the multi-material three-dimensional printing it is possible to now integrate the paraserial fiber tissue through a more flexible material. This material composition constrains the ranges of motion very closely to the biological model.

Results and Discussion

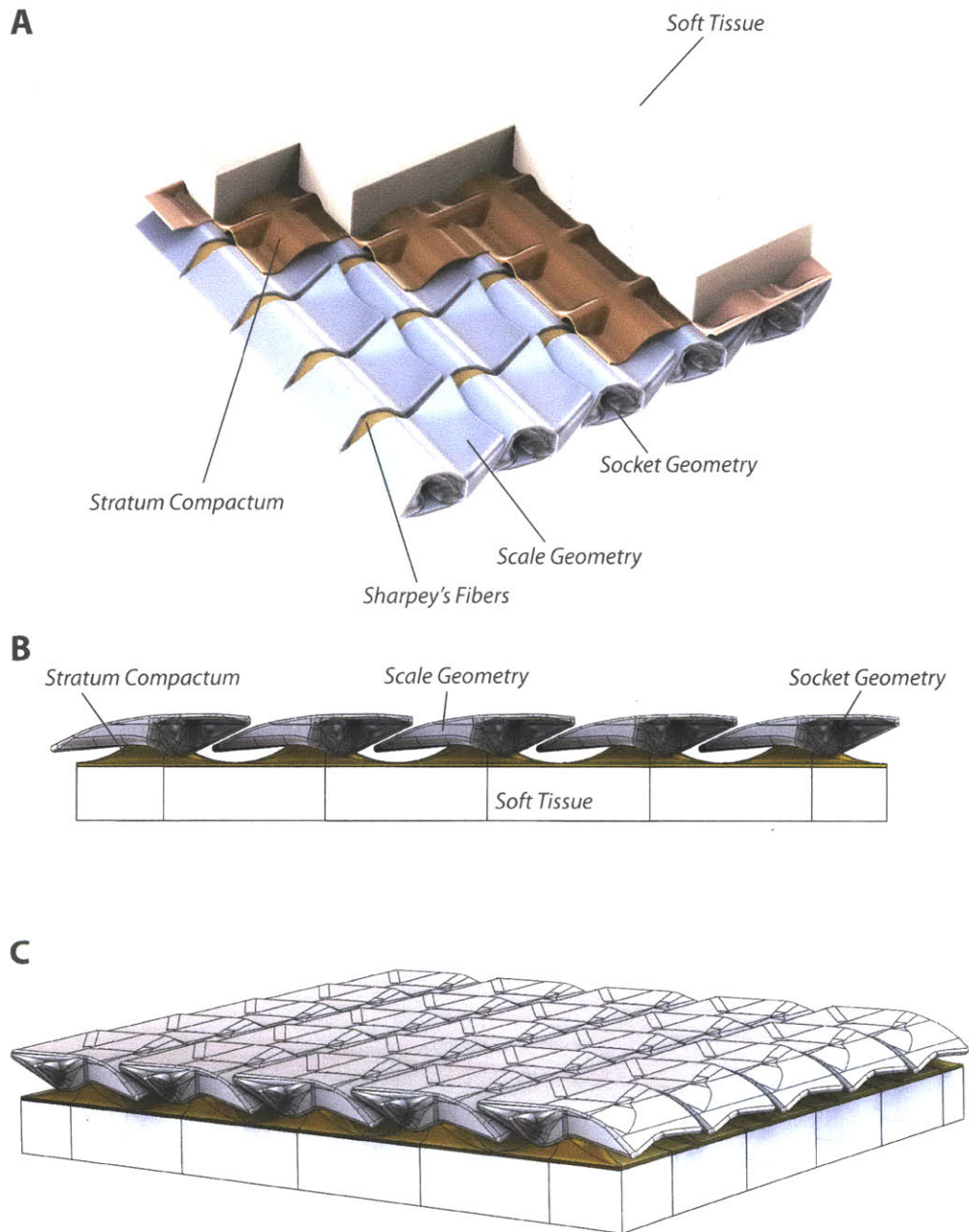


Figure 46: The final virtual assembly incorporating the scale geometry, paraserial callagenous connection, the underlying stratum compactum and the inner soft tissue. (A) Interior view with partially disassembled to show the different layers of the design; (B) from side perspective displaying the overlapping interface with interserial stratum compactum connection; (C) The exterior perspective showing the modular character of the virtual model.

Results and Discussion

The entire design assembly is constructed with an emphasis on modularity (Figure 46B-C). Self-similar modules of scale-, stratum compactum, Sharpey's fibers and soft tissue can be assembled to infinite planar assemblies.

Multi-Material Prototype Evolution

To calibrate the right amount of flexibility, several 2 x 2 scales assemblies have been prototyped varying the thickness and hardness of the connective tissue (Figure 47, 48 and 49). Finally, the composition of the highly flexible material TangoPlus in combination with a connective tissue thickness of 7mm (3.5mm stratum compactum + 3.5mm soft tissue) was chosen for the final 5 x 5 scales prototype.

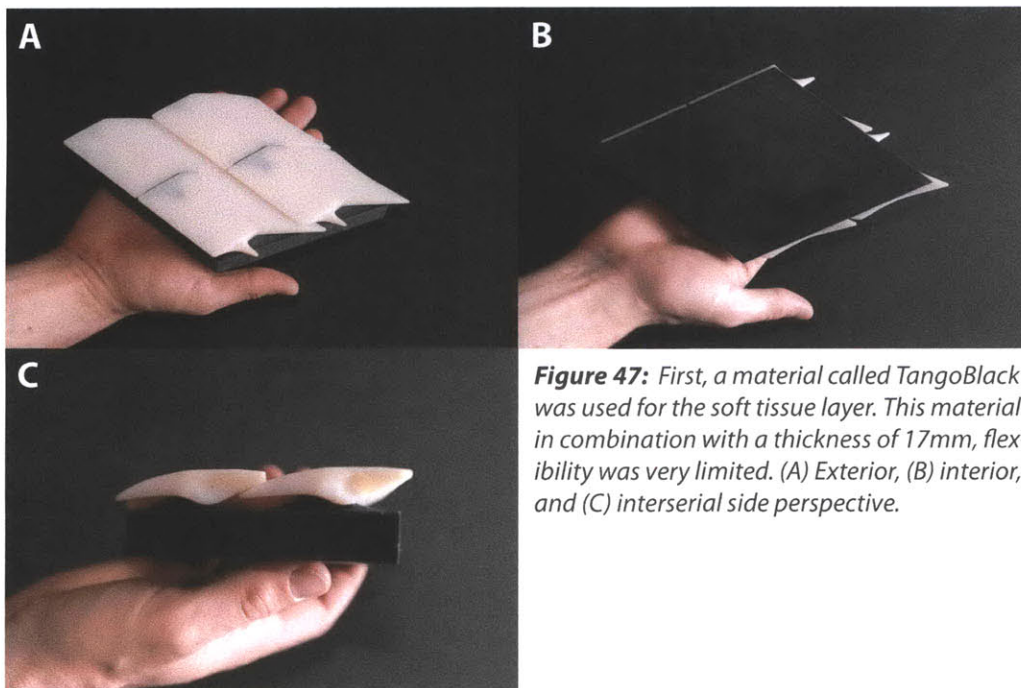


Figure 47: First, a material called TangoBlack was used for the soft tissue layer. This material in combination with a thickness of 17mm, flexibility was very limited. (A) Exterior, (B) interior, and (C) interserial side perspective.

Results and Discussion

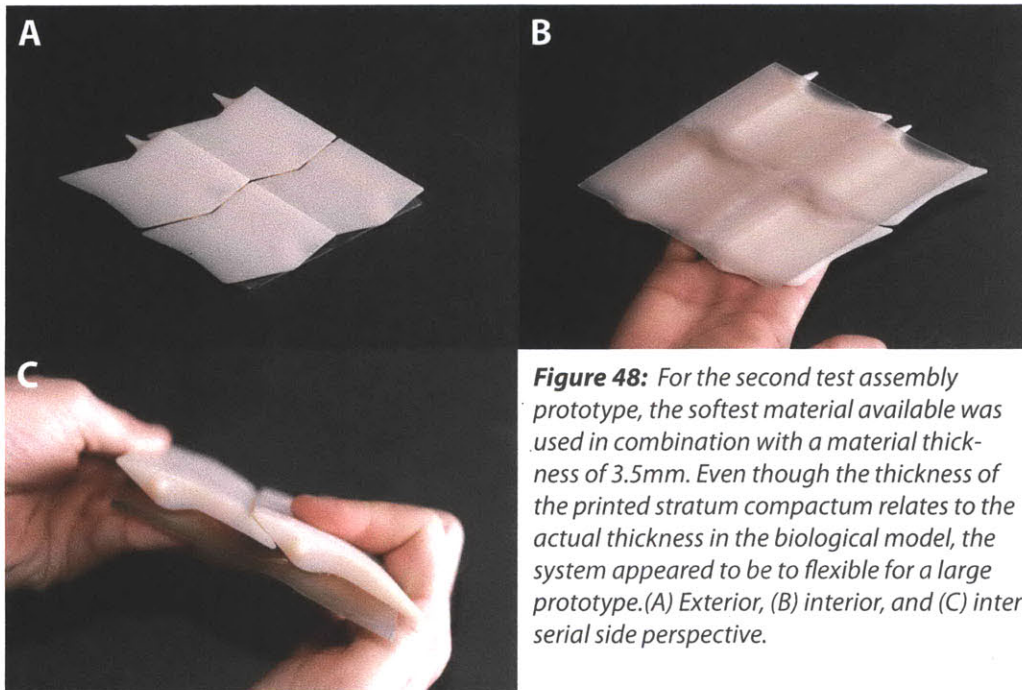


Figure 48: For the second test assembly prototype, the softest material available was used in combination with a material thickness of 3.5mm. Even though the thickness of the printed stratum compactum relates to the actual thickness in the biological model, the system appeared to be to flexible for a large prototype. (A) Exterior, (B) interior, and (C) interserial side perspective.

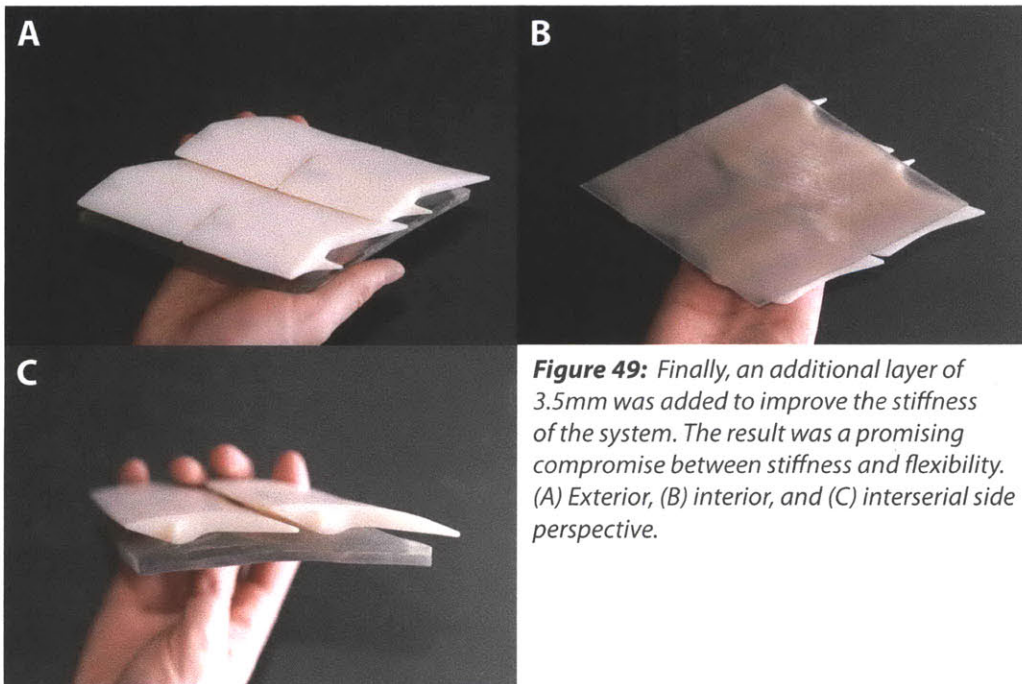


Figure 49: Finally, an additional layer of 3.5mm was added to improve the stiffness of the system. The result was a promising compromise between stiffness and flexibility. (A) Exterior, (B) interior, and (C) interserial side perspective.

Results and Discussion

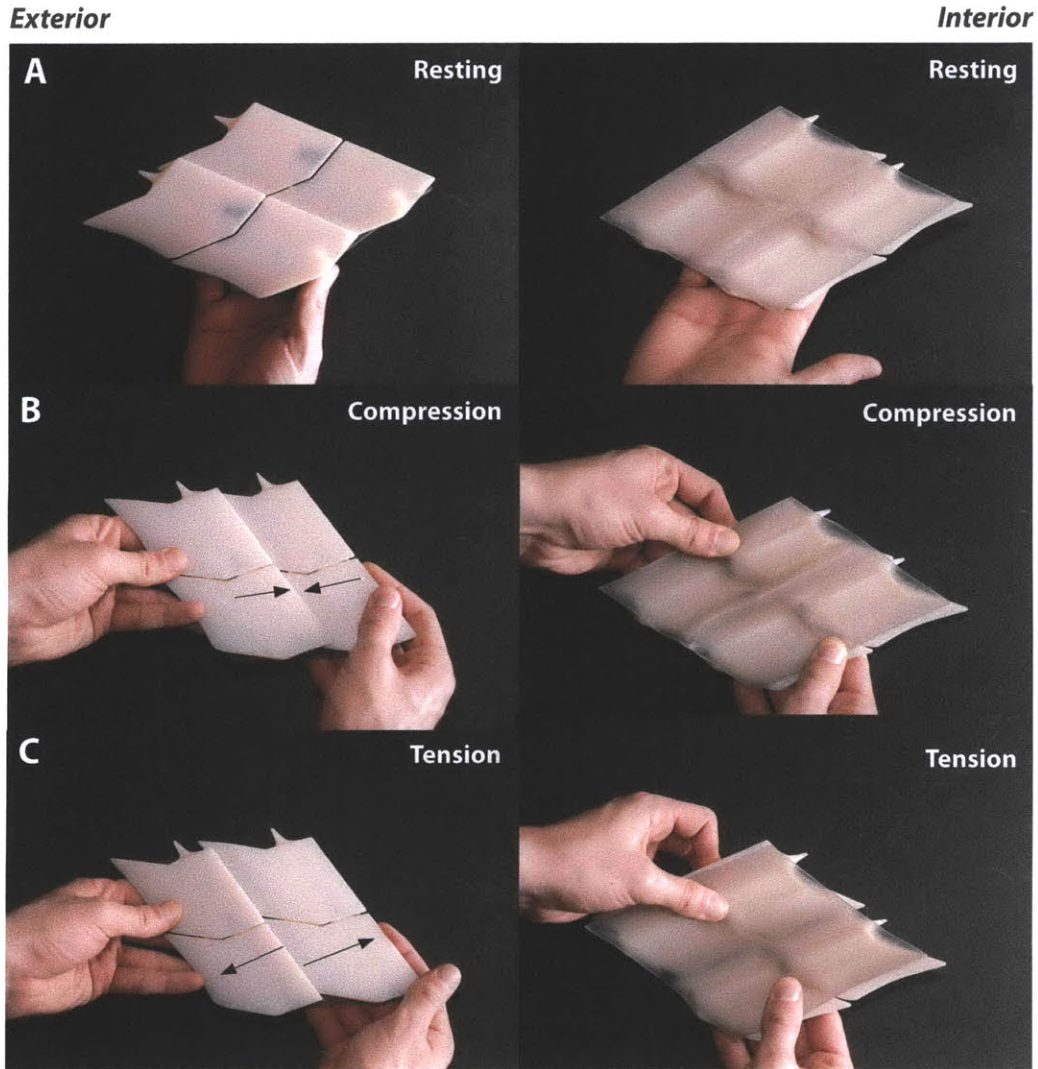


Figure 50: The multi-material 2 x 2 test prints show very similar degrees of freedom within the macroscale assembly. (A) Scale assembly in resting position; (B) scale assembly in compression state; (C) scale assembly in tension state. (Compare to Figure 38 and 39)

Results and Discussion

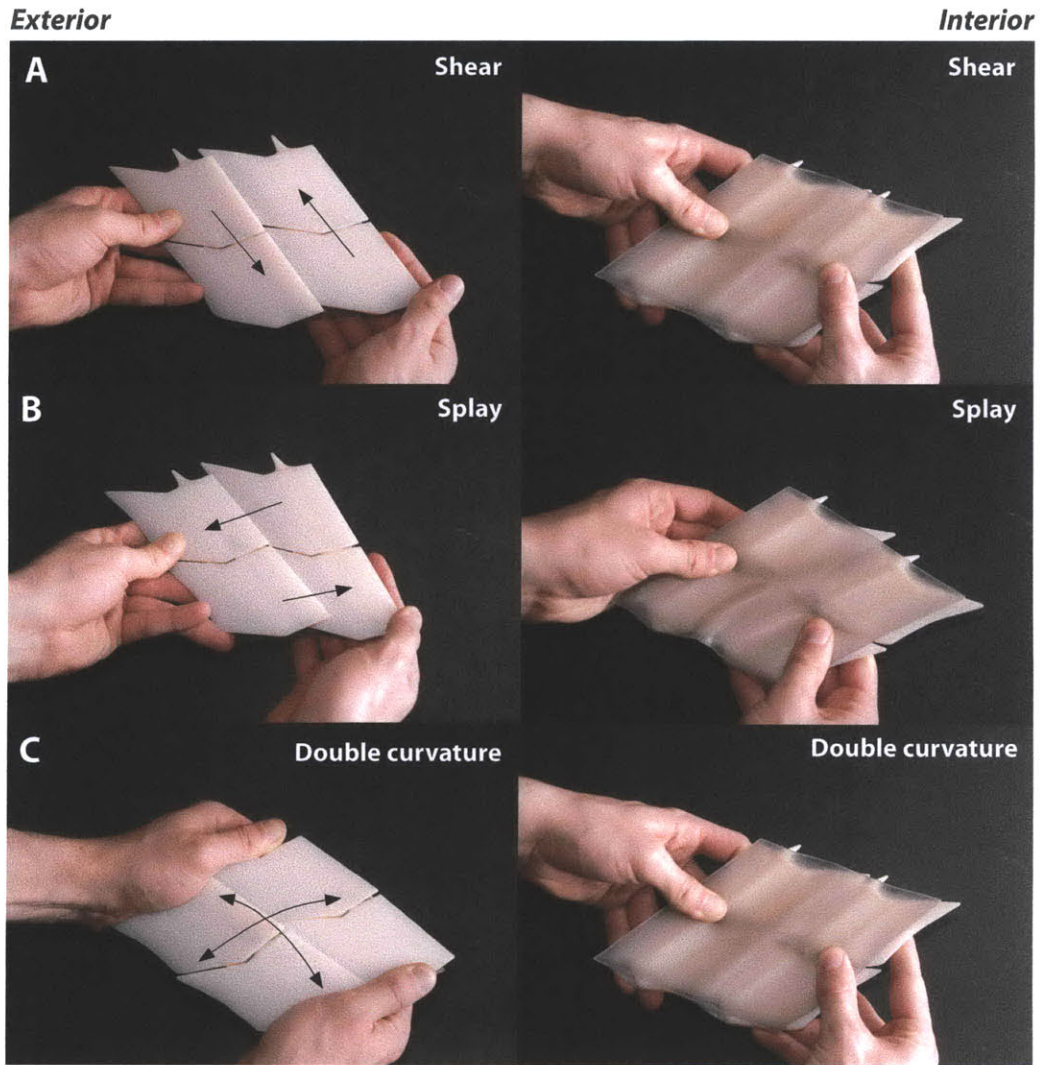


Figure 51: (A) Scale assembly in shear situation; (B) scale assembly in splay situation; (C) scale assembly performing double curvature. (Compare to Figure 40, 41, and 42)

Results and Discussion

Final Functional Multi-Material Prototype

The final prototype consists of a 5 x 5 assembly of 25 scales (Figure 53). Like the biological system of *P. senegalus*, it possesses flexible connections in paraserial directions as well as a flexible connective tissue layer underneath (interior) connecting each single scale along the axial ridge.

The prototype shows as desired very flexible behavior in the interserial direction (Figure 53), while the paraserial flexibility is restricted through the peg-and-socket joint and simulated Sharpey's fiber connection, although completely constrained (Figure 54A).

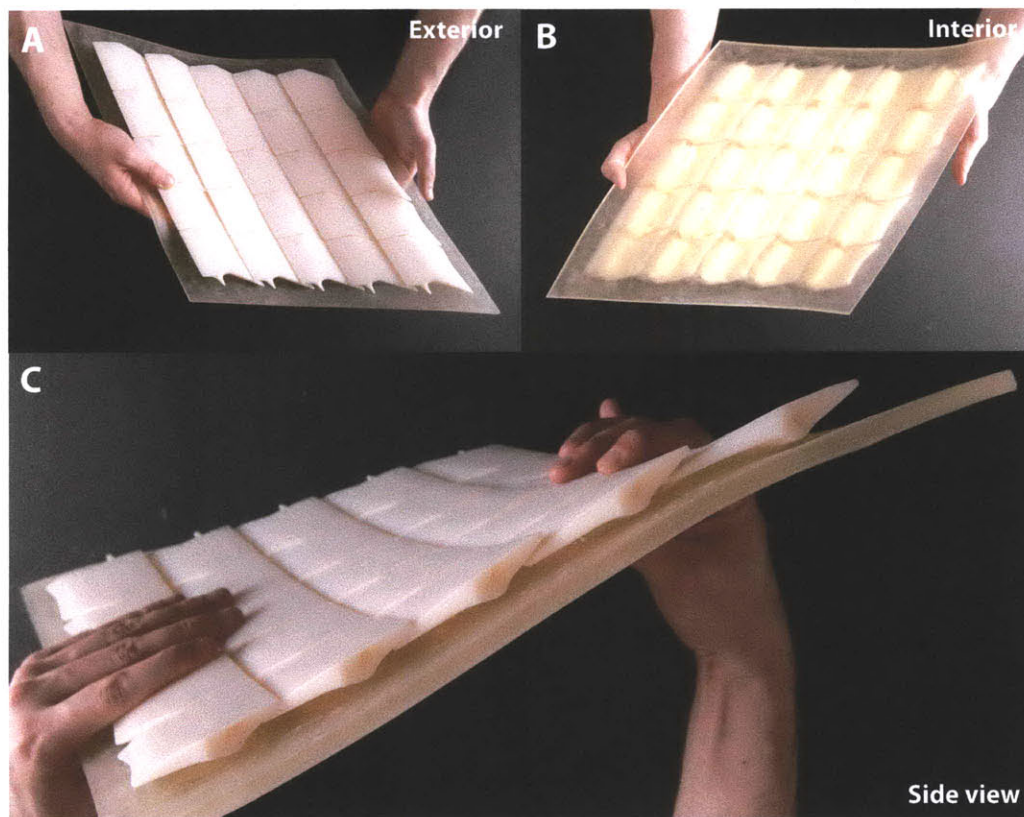


Figure 52: Final performative, multi-material prototype consisting out of 25 scales (5 x 5 scale assembly). (A) Exterior, (B) interior, (C) and side view.

Results and Discussion

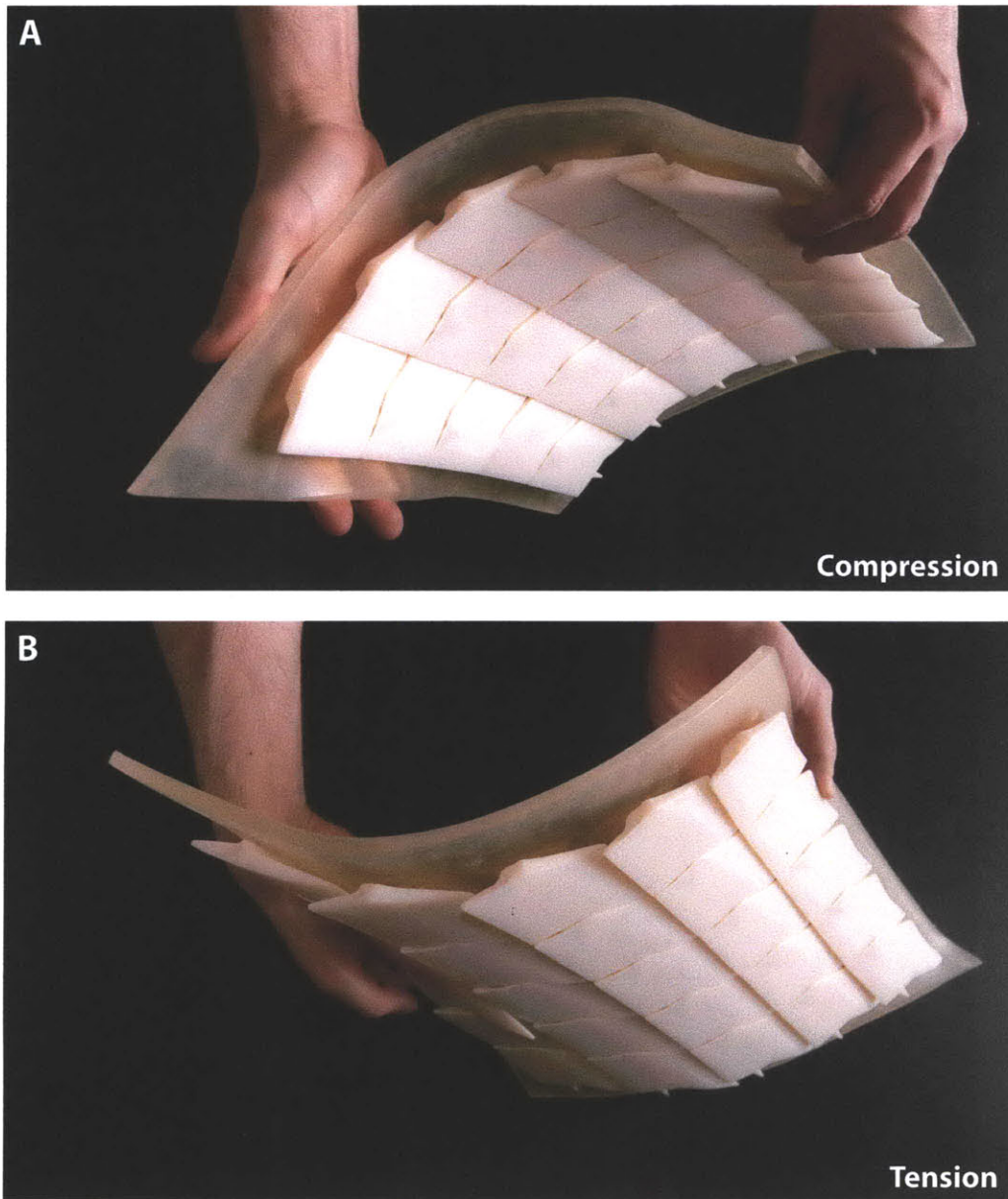


Figure 53: Final prototype (A) in compression state simulating *P. senegalus* body position with largest body curvature and (B) in tension state simulating the opposite body region while being under large curvature.

Results and Discussion

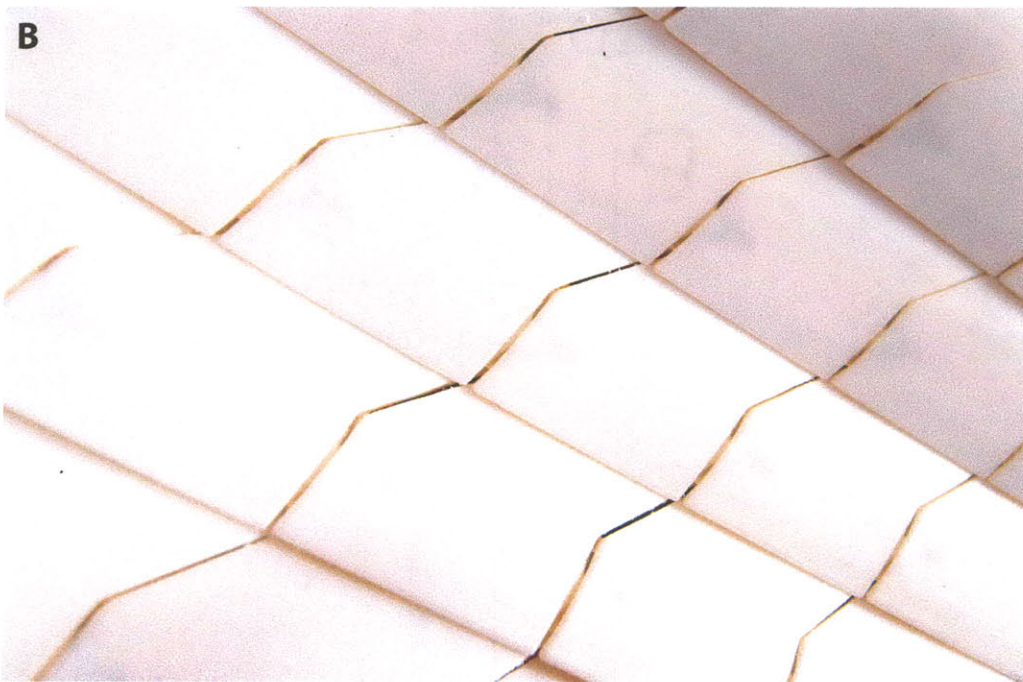
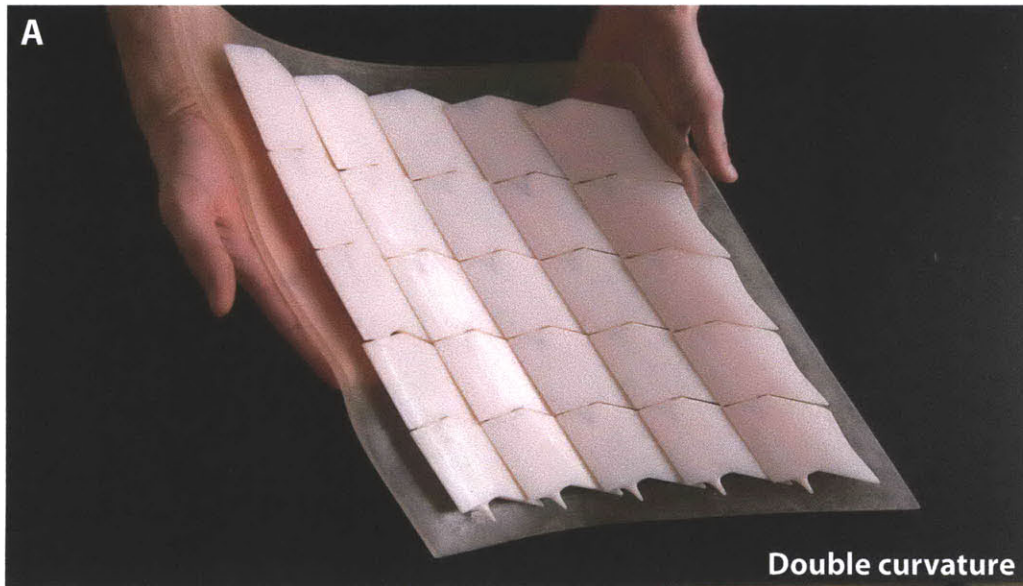


Figure 54: (A) Final Prototype performing double curvature. (B) Close-up of exterior scale appearance.

Results and Discussion

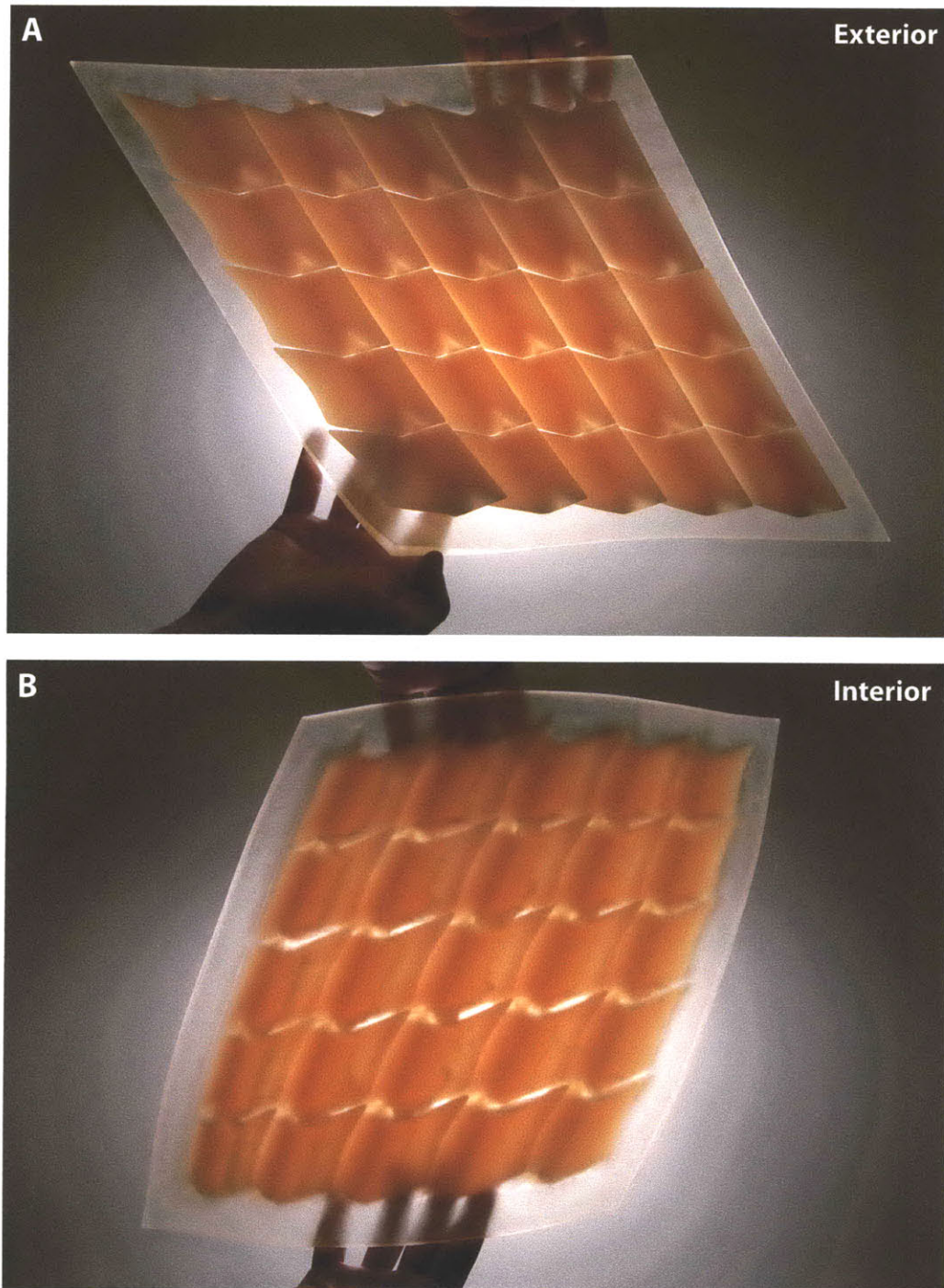


Figure 55: Showing translucency of final prototype from (A) exterior and (B) interior view.

Results and Discussion

Table of Abstracted Design Principles

Materiality



↑
Quadlayered Composite of Polypterus

Role:

Local protection (penetration, scratch and wear resistance)

Tessellation



↑
Skull of Polypterus

↑
Body Scales of Polypterus

↑
Scales around Pectoral Fins

Role:

Balance protection (high L) and flexibility (low L)

Joint Systems



↑
Paraserial Peg-and-Socket Joint

↑
Interserial Overlap

Role:

Controls unit to unit range of motion and contributes to global biomechanical flexibility and stress distribution

Global Counter Helix



↑
Mirrored Helical Distribution of Scales

Role:

*(1) Self-stabilizing system (max. volume at $\phi = 54.44^\circ$)
(2) Mirrored helical arrangement provides anisotropic ranges of biomechanical motion of entire fish*

Constructive Complexity



↑
Main Body Scales

↑
Specialized Scales

Role:

Heterogeneous design solutions need custom elements

Table 3: Table presenting abstracted design principles for application oriented scale assembly designs

Additional Abstraction from Biological System

The presented fish armor of *P. senegalus* is an inspiring example of how nature combines form with function. Every geometric feature appears to have a very specific task resulting in a highly performative whole. But since the design of the biological armor is focused on following the shape and motions of the fish, it is necessary to identify steps of abstraction to utilize the extracted design principles for different kinds of applications:

1. Constructive Complexity

The fish only possesses specialized joining scales in the most dorsal and ventral location of its squamation connecting two mirrored half turned helical scale rows. To be able to produce a wider range of very different shapes including shapes, e.g. corners, new special scales need to be invented. This invention can be very close to the actual design of the scale but also very different depending on the application or goal of geometry.

2. Different materials need adjusted designs

Biological organisms possess a very unique and very different way to produce their shapes. Biological shapes grow, which means they increase in size and change shape over time; also, they can self-repair. It is very difficult if not impossible to simulate and utilize the process of growth for commercial product purposes. For that reason, a very different range of materials and fabrication processes occur. While in the past most processes have been subtractive (cutting, milling, etc.), new additive fabrication techniques like 3D printing are much closer to the biological ideal. Very complex and even different materials can be combined into a functional whole. But so far, only a very different material range is available, performing in very different ways. Especially the widely used fibrous composite materials are very difficult and so far not integrated into 3D printing processes. These different available materials with their very different performance characteristics need to be incorporated into the design process and the design result and can lead to radically different design decisions.

Results and Discussion

3. Design based on functional performance

A very promising way to build a hierarchical design model for customized kinetic scale structures is achieved by starting with a kinetic diagram of allowable motions. These allowable motions can be represented through defining the extreme conditions of each degree of freedom and each range of motion. If a kinetic design component is decomposed in functional geometric features that are related to degrees of freedom, each geometric feature of a scale within a squamation can be informed by the conditions of extreme curvature to make a computational discrete design system. The articulation of the system is therefore mainly informed by its functional performance.

Contributions

Contributions

This thesis presented three main contributions that have been achieved:

First, a framework of how to design with biological inspiration was presented, including techniques of model making. Complex systems were captured through decomposition into smaller problems. Morphometric analysis were utilized to understand complex geometry of biological shapes. Furthermore, methods of processing μ CT data , implementing morphometrics into CAD solutions, automation of measurement techniques, and different 3D printing fabrication techniques including multi-material printing were implemented.

The second major contribution was the development of a parametric scale design structure containing all extracted information of proportion and functionality. Physical prototypes were produced using different fabrication techniques.

Last, new biological design principles were extracted, abstracted and transferred into general design principles for future performance-based scale structure investigations.

Future Work

Future Work

It will be highly interesting to explore the differentiation of scale geometry along the fish body in more detail. Extensive microcomputed tomography could be used to scan the whole fish squamation. With the help of morphometric analysis the shape differences can be displayed and mapped as functional gradients in geometry to functional behavior of a system.

Also, different fabrication techniques would be interesting to explore to produce self-similar scales or even differentiated scales at a lower cost. But also, the combination of 3D printing and pultrusion processes could be of high interest to generate solid scales with fibrous connections. Especially integrated fibrous connections are only very difficult to fabricate synthetically.

Finally, it would be my desire to develop a scale design for a specific application.

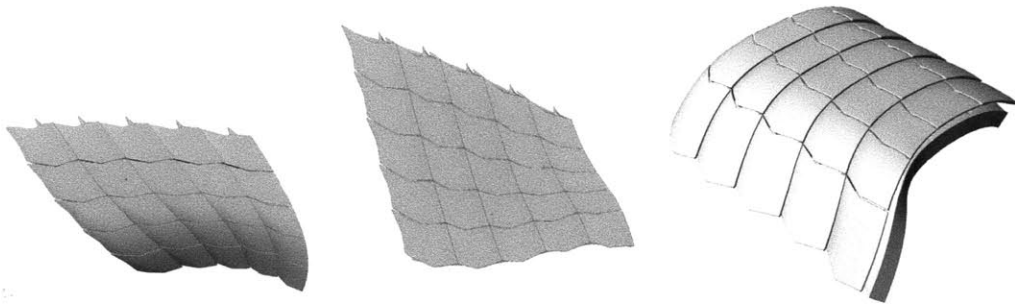


Figure 56: *Distorted scale integuments.*

Bibliography

- Arciszewski, Tomasz, and Joanna Cornell. 2006. Bio-inspiration: Learning Creative Design Principia. In *Intelligent Computing in Engineering and Architecture*, 32-53. http://dx.doi.org/10.1007/11888598_5.
- Bertalanffy, Ludwig Von. 1976. *General System Theory: Foundations, Development, Applications*. Revised. George Braziller, March.
- Bookstein, F. L. 1997. *Morphometric Tools for Landmark Data: Geometry and Biology*. Rev and Expande. Cambridge University Press, June 28.
- Brainerd, Elizabeth L. 1994. Mechanical design of polypterid fish integument for energy storage during recoil aspiration. *Journal of Zoology* 232, no. 1: 7-19. doi:10.1111/j.1469-7998.1994.tb01556.x.
- Britz, R., and P. Bartsch. 2003. The myth of dorsal ribs in gnathostome vertebrates. *Proceedings of the Royal Society B: Biological Sciences* 270, no. 0 (8): S1-S4. doi:10.1098/rsbl.2003.0035.
- Bruet, Benjamin J. F. Multiscale structural and mechanical design of mineralized biocomposites. Thesis, Massachusetts Institute of Technology. <http://dspace.mit.edu/handle/1721.1/44200>.
- Bruet, Benjamin J. F., Juha Song, Mary C. Boyce, and Christine Ortiz. 2008. Materials design principles of ancient fish armour. *Nat Mater* 7, no. 9: 748-756. doi:10.1038/nmat2231.
- Clark, R. B., and J. B. Cowey. 1958. Factors Controlling the Change of Shape of Certain Nemertean and Turbellarian Worms. *J Exp Biol* 35, no. 4 (December 1): 731-748.
- Daget, Jacques, Mireille Gayet, François J Meunier, and Jean-Yves Sire. 2001. Major discoveries on the dermal skeleton of fossil and Recent polypteriforms: a review. *Fish and Fisheries* 2, no. 2: 113-124. doi:10.1046/j.1467-2960.2001.00046.x.

Bibliography

- Dryden, I. 1999. . In *Stochastic geometry*, ed. Ole E. Barndorff-Nielsen, W. S. Kendall, and M. N. M. Van Lieshout, 333-364. CRC Press.
- Filler, Aaron G. 2007. *The Upright Ape: A New Origin of the Species*. New Page Books, July.
- Gans, Carl. 1980. *Biomechanics: An Approach to Vertebrate Biology*. University of Michigan Press, October 1.
- Gemballa, Sven, and Peter Bartsch. 2002. Architecture of the integument in lower teleostomes: functional morphology and evolutionary implications. *Journal of Morphology* 253, no. 3 (September): 290-309. doi:10.1002/jmor.10007.
- Goodman, Nelson. 1978. *Ways of Worldmaking*. New Ed. Hackett Publishing Co, Inc, November.
- Holland, John. 1996. *Hidden Order: How Adaptation Builds Complexity*. First Edition. Basic Books, September 3.
- Kendall, D. G., D. Barden, T. K. Carne, and H. Le. 1999. *Shape and Shape Theory*. 1st ed. Wiley, October 25.
- Kendall, David G. 1989. A Survey of the Statistical Theory of Shape. *Statistical Science* 4, no. 2: 87-99.
- Krohs, Ulrich, and Peter Kroes. 2009. *Functions in Biological and Artificial Worlds: Comparative Philosophical Perspectives*. The MIT Press, March 31.
- Long, J, M Hale, M Mchenry, and M Westneat. 1996. Functions of fish skin: flexural stiffness and steady swimming of longnose gar, *Lepisosteus osseus*. *J Exp Biol* 199, no. 10 (October 1): 2139-2151.
- Nachtigall, Werner. 2003. *Bau-Bionik: Natur, Analogien, Technik*. 1st ed. Springer, Berlin, February 17.

Bibliography

- Ortiz, Christine, and Mary C. Boyce. 2008. MATERIALS SCIENCE: Bioinspired Structural Materials. *Science* 319, no. 5866 (February 22): 1053-1054. doi:10.1126/science.1154295.
- Ørvig, T. 1967. Phylogeny of tooth tissues: Evolution of some calcified tissues in early vertebrates. *Structural and Chemical Organization of Teeth*.
- Pearson, D. M. 1981. Functional aspects of the integument in polypterid fishes. *Zoological Journal of the Linnean Society* 72, no. 1: 93-106. doi:10.1111/j.1096-3642.1981.tb01653.x.
- Pearson, D. M. 1982. Primitive bony fishes, with especial reference to Cheirolepis and palaeonisciform actinopterygians. *Zoological Journal of the Linnean Society* 74, no. 1: 35-67. doi:10.1111/j.1096-3642.1982.tb01140.x.
- Ryder, John A. 1892. On the Mechanical Genesis of the Scales of Fishes. *Proceedings of the Academy of Natural Sciences of Philadelphia* 44: 219-224.
- Schaefer, Frank. 2004. *Aqualog: Polypterus--Bichirs*. Hollywood Import & Export, Inc., April 30.
- Schroeder, Karsten. 1989. Die Struktur des Schuppenpanzers von *Lepisosteus* und seine Function aus biomechanischer Sicht. Universität Tübingen.
- Simon, Herbert A. 1996. *The Sciences of the Artificial - 3rd Edition*. 3rd ed. The MIT Press, October 1.
- Sire, Jean-Yves [1]. 1989. From Ganoid To Elasmoid Scales in the Actinopterygian Fishes*). *Netherlands Journal of Zoology* 40: 75-92. doi:10.1163/156854289X00192.
- Stiny, George. 2008. *Shape: Talking about Seeing and Doing*. The MIT Press, March 31.

Bibliography

Thompson, D'Arcy Wentworth, and Kroonm Thompson. 1992. *On Growth and Form: The Complete Revised Edition*. Revised. Dover Publ Inc, June.

Tytell, Eric D., and George V. Lauder. 2002. The C-start escape response of *Polypterus senegalus*: bilateral muscle activity and variation during stage 1 and 2. *J Exp Biol* 205, no. 17 (September 1): 2591-2603.

Wang, Lifeng, Juha Song, Christine Ortiz, and Mary C. Boyce. 2009. Anisotropic design of a multilayered biological exoskeleton. *Journal of Materials Research* 24, no. 12 (12): 3477-3494. doi:10.1557/jmr.2009.0443.

Weisstein, Eric W. Euler Angles -- from Wolfram MathWorld. Text. <http://mathworld.wolfram.com/EulerAngles.html>.

Zelditch, Miriam L., Donald L. Swiderski, David H Sheets, and William L. Fink. 2004. *Geometric Morphometrics for Biologists*. 1st ed. Academic Press, July 15.